UNIVERSIDADE FEDERAL DO CEARÁ
CENTRO DE CIÊNCIAS
DEPARTAMENTO DE FÍSICA
PROGRAMA DE PÓS-GRADUAÇÃO EM FÍSICA

FELIPE GIOACHINO OPERTI

INTERPOLATION STRATEGY BASED ON DYNAMIC TIME WARPING

FORTALEZA

2015

FELIPE GIOACHINO OPERTI

INTERPOLATION STRATEGY BASED ON DYNAMIC TIME WARPING

Presented by Programa de Pós-Graduação em Física da Universidade Federal do Ceará, as partial requirement for the acquisition of the licence of Mestre em Física. Field: Physics of Condensed Matter.

Orientador: Prof. Dr. José Soares de Andrade Júnior

FORTALEZA

2015

FELIPE GIOACHINO OPERTI

INTERPOLATION STRATEGY BASED ON DYNAMIC TIME WARPING

Presented by Programa de Pós-Graduação em Física da Universidade Federal do Ceará, as partial requirement for the acquisition of the licence of Mestre em Física. Field: Physics of Condensed Matter.

Approved in 29/01/2015

EXAMINERS

Prof. Dr. José Soares de Andrade Júnior (Orientador)
Universidade Federal do Ceará (UFC)

Dr. Erneson Alves de Oliveira
Universidade Federal do Ceará (UFC)

Prof. Dr. Liacir Dos Santos Lucena
Universidade Federal do Rio Grande do Norte (UFRN)

International data for the publication
Universidade Federal do Ceará
Biblioteca Setorial de Física

A000p Operti, Felipe Gioachino .
Interpolation strategy based on Dynamic Time Warping / Felipe Gioachino Operti. – 2015.
53 p.;il.

Dissertação de Mestrado - Universidade Federal do Ceará, Departamento de Física, Programa de Pós-Graduação em Física, Centro de Ciências, Fortaleza, 2015.
Área de Concentração: Física da Matéria Condensada
Orientação: Prof. Dr. José Soares de Andrade Júnior

1. Dijkstra's Algorithm. 2. Optimal-Path. 3. Dynamic Time Warping. 4. Standard Linear Interpolation. 5. Dynamic Time Warping Interpolation. I.

CDD:000.0

To my parents, my family and to my love Lorena...

Acknowledgments

I would like to thank everyone who contributed to the thesis. In particular:

- First and foremost, my parents;
- Professor Dr. José Soares de Andrade Júnior for his orientation, his help and his support during this year and a half;
- Dr. Erneson Alves de Oliveira that with a lot of calm and patience supported me countless times;
- Rilder Pires for his help in programming;
- Samuel Morais for the many tips;
- Thiago Bento for the many discussions;
- Caleb Alves for his incentives;
- Tatiana Alonso Amor for her friendship;
- The Department of Physics (UFC), all the professors and the colleagues of the group of complex systems;
- CNPq for the financial support;
- My italian friends, Nicoló, Simone and Alessandro for their tips;
- My love, Lorena for her empathy.

I want to know how God created this world. I am not interested in this or that phenomenon, in the spectrum of this or that element. I want to know his thoughts; the rest are details.
Albert Einstein

ABSTRACT

In oil industry, it is essential to have the knowledge of the stratified rocks' lithology and, as consequence, where are placed the oil and the natural gases reserves, in order to efficiently drill the soil, without a major expense. In this context, the analysis of seismological data is highly relevant for the extraction of such hydrocarbons, producing predictions of profiles through reflection of mechanical waves in the soil. The image of the seismic mapping produced by wave refraction and reflection into the soil can be analysed to find geological formations of interest. In 1978, H. Sakoe et al. defined a model called Dynamic Time Warping (DTW)[23] for the local detection of similarity between two time series. We apply the Dynamic Time Warping Interpolation (DTWI) strategy to interpolate and simulate a seismic landscape formed by 129 depth-dependent sequences of length 201 using different values of known sequences m, where $m = 2, 3, 5, 9, 17, 33, 65$. For comparison, we done the same operation of interpolation using a Standard Linear Interpolation (SLI). Results show that the DTWI strategy works better than the SLI when $m = 3, 5, 9, 17$, or rather when distance between the known series has the same order size of the soil layers.

Keywords: Dijkstra's Algorithm. Optimal-Path. Dynamic Time Warping. Standard Linear Interpolation. Dynamic Time Warping Interpolation.

LIST OF FIGURES

LIST OF ACRONYMS

ABNT	Associação Brasileira de Normas Técnicas
CNPq	Conselho Nacional de Desenvolvimento Científico e Tecnológico
OP	Optimal path
OPW	Optimal path warping
DTW	Dynamic Time Warping
SLI	Standard Linear Interpolation
DTWI	Dynamic Time Warping Interpolation

SUMMARY

1 INTRODUCTION

The field of complex systems is extremely wide. It encloses different areas of research, such as biology, sociology, finance and geology [1, 2, 3, 4]. The relations between these areas consist on the fact that all of them are made by parts connected, as the brain system is made of neurons, or a social network is made by people. The study of this "complex" connections is the aim of a complex systems researcher, in order to find the collective behaviors of given system. Despite being a modern field of research, it is difficult to determine when these studies first took place. *Science* paper, entitled "How long is the coast of the Britain? Statistical Self-similarity and fractional dimension", published by the mathematician Benoit B. Mandelbrot in 1967 [5]. He explained how complicated is to measure a coast of a country, in particular the coast of Britain which has a lot of inlets. Mandelbrot cited the work of Richardson 1961 where he observed that the length depends on the scale of the measure. The Richardson's formula is,

$$L(G) = FG^{1-D}, \tag{1.1}$$

where G is a positive scale, F is a positive pre-factor and D is a constant, called the dimension. Richardson defined D as a "characteristic" of a frontier. For the coast of Britain, $D = 1.25$, and naturally, L is the approximated length of the coast.

The stratifications of rocks also can be studied using fractal models [6][7][8]. The interpretation of the stratigraphic sequences is very important in a lot of fields such as earth history or resources extraction [6]. The *self-affinity*, one of the fractals main feature, is a characteristic of stratified rocks, therefore it is possible to apply fractal models to better understand the structure of rocks in terms of their sections, that mathematically are converted into sequences. A section is a vertical sequence of a rock, geometrically represented by a vertical line segment with topological dimension 1. It is possible to plot the line above in the presence or not of some properties like density, resistivity or the presence of a particular fossil. For example, if it occurs only once in the sequence, the fractal dimension is 0. If it appears at all points of the sequence, the fractal dimension is

1, and if it appears in some points, the fractal dimension of the set will be between 0 and 1. That also could be treated as a sequence of sediments deposited during a particular periods of time. This mathematical approach based on fractal geometry can be used to study the lithology of stratified rocks.

This thesis is organized as follows: In Chapter 2, we present some theoretical foundations of the science of *Fractals* that played an important role in the geometry of last century. We introduce the traditional concept of the *Hausdorff-Besicovith dimension* and its relation with the *fractal dimension*, the *self-similarity* and *self-affinity*. Some elementary notions about the *percolation theory* are then presented, introducing the *forest fire model* and the*percolation model* with some hints to its application in oil field. Some elements of *graph theory* are presented, introducing the *shortest path problem* with its numeral solution, the *Dijkstra's algorithm*.

In Chapter 3, we presented in details a method that was born from the *spoken word recognition*, called *Dynamic Time Warping* (DTW), and was an inspiration to our interpolation strategy. Moreover, we also showed the results of our method applied to seismic data, in order to predict the lithology of stratified rocks and make comparisons with standard technique.

Finally, we conclude this dissertation making some conjectures as well as some perspectives for future projects.

2 THEORETICAL FOUNDATIONS

Benoit B. Mandelbrot started his book, *The Fractal Geometry of Nature*, written in 1982, with the following phrase:

> "Why is geometry often described as "cold" and "dry"?"
>
> — Benoit B. Mandelbrot

In a few words, Mandelbrot discovered that the Nature is "not that simple". Actually, it is a complex world which the Euclidian geometry cannot explain properly in its totality and, in order to describe that world, he introduce the fractal theory. In this chapter, we introduce the theoretical foundations of the complex systems presenting an introduction to fractal theory and percolation theory. After that, we explain some concepts of the graph theory, including the shortest path problem with its computational solution, the Dijkstra's algorithm.

2.1 Introduction to Fractal Theory

2.1.1 What is a Fractal?

The word *Fractal* was coined by B. B. Mandelbrot in 1975 in his book *Les Objects Fractals: Forme, hasard et dimension* [11]. Mandelbrot described some pure mathematical objects, as *Koch snowflake*, *Peano curve* and many others, which in those years were considered extremely far from reality, appearing in the nature. He created a new kind of geometry to explain the shapes in our world. In fact, the classical geometry, the *Euclidean geometry*, is made out of perfect shapes, such as points, lines and planes, even though nature is not that perfect, it can be, in fact, more complex and made of strange objects. In this section, we present the main contributions of Mandelbrot, some concepts and models related with fractals.

As Mandelbrot explained in his another book, *The Fractal Geometry of Nature* [9], the word *fractal* was chosen by him referring to the latin word *fractus* that means "irregular" and the relative verb *frangere* that means "to break". In this way, when we speak about *natural fractal* we think of a natural structure that is easily representable by a fractal set like a Brownian curve from a Brownian motion.

A fractal could be defined as an object that has the same pattern under a change of scale [12]. In nature, there are some examples: A river and its tributaries or the branching of trees and their roots and, also, a coastline with its multitude of inlets and peninsulas. Another clear example is the Fern leaf, where each leaf branch is similar to the entire leaf. This is the main characteristic of fractals and it is called "self-similarity". The Fig. 1 shows the *Mandelbrot set*, .a famous fractal studied and popularized by Mandelbrot and fractal examples existing in nature

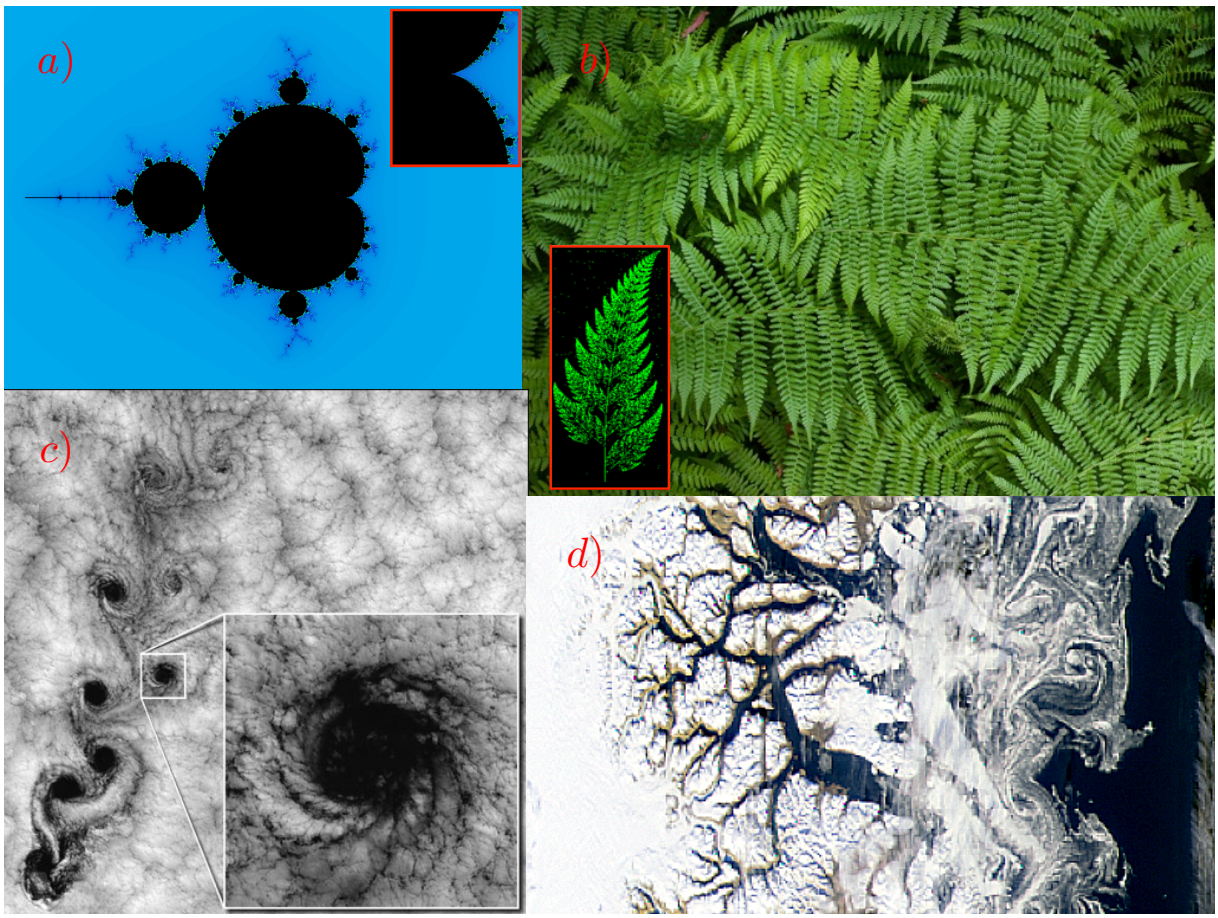

Figure 1: The Fig. *a* shows the *Mandelbrot set* with a zoom in a part of it. In Fig. *b*, an image of a fern made available by the National Geographic, with a simulation of a fern leaf. Fig. *c* and *d* are two images made available by NASA; the first one shows a large-scale fractal motion of clouds and the second image shows the fractal patterns of the fjords of the Greenland.

2.1.2 Hausdorff-Besicovith dimension

A much accurate definition of fractals was given by Mandelbrot:

"*A fractal is by definition a set for which the Hausdorff-Besicovitch dimension strictly exceeds the topological dimension.*"

In the context of the *Euclidean geometry*, the topological dimension gives us an intuitive idea of the object and that dimension is an integer number. However, in case of *fractals*, it does not necessarily give us an intuitive representation. For instance, the topological dimension of the Cantor set is 0 and its Hausdorff-Besicovith dimension is 0.6309. The Hausdorff-Besicovitch dimension is defined for a set of points S as a critical dimension where M_l of this set changes from 0 to ∞,

$$M_l = \sum h(l) = \sum \gamma(l)\delta^l = \lim_{\delta \to 0} \gamma(l) N(\delta)\delta^l \to \begin{cases} 0 & if\ l > D, \\ \infty & if\ l < D, \end{cases} \tag{2.1}$$

where $N(\delta)$ is the necessary number of test function $h(l)$ to complete the S set, $\gamma(l)$ is a geometric factor, l is the dimension of the measure and δ is the measured object's length of the test function.

Here we mention two methods to calculate $N(\delta)$: The *box counting method* and the *yardstick method*. Using the *box counting method*, we divide the landscape in boxes of length δ. If $\delta \to 0$, we have,

$$N(\delta) \sim \frac{1}{\delta^D}. \tag{2.2}$$

We also could find $N(\delta)$ using the *yardstick method*. It consists in trying to delimitate the perimeter of the figure with segments of the same dimension δ. In this case we have a similar expression:

$$N(\delta) \sim \frac{1}{\delta^D}. \tag{2.3}$$

In the field of Complex Systems, the Hausdorff-Besicovith dimension is usually called the Fractal dimension. In 1967, Mandelbrot used the *yardstick method* to calculate the Hausdorff-Besicovith dimension, or fractal dimension, of the west coast of Britain and obtained $D = 1.25$ [5].

2.1.3 Self-similarity and Self-affinity

We define fractals as self-similar objects; in other words, an object that has the same pattern under a change of scale. A *self-similar transformation* or *isotropic transformation* is a transformation that begins from a space of E-dimension with the following point $x = (x_1, ..., x_E)$ to the same space of E-dimension with the following new point $x' = (rx_1, ..., rx_E)$, where r is the scale factor [14]. This is an isotropic transformation due to the scale factor r that does not depend on the coordinates (it is always the same). Pure geometrical objects, like the *Koch snowflake* or the *Cantor set*, are self-similar. Their structures do not change with different scales as well as their *fractal dimensions*.

Are all the fractal self-similar? A. Lakhtakia *et al.* tried to answer this question in their paper [7]. The answer is no. They argued that there is another feature of fractals called *self-affinity* and the *self-similarity* is only a special case of this property. To understand it, they provided a variant of the question: how long is the coastline of continental Europe, excluding all islands? The fractal dimension of the coastlines of France, Spain and Portugal are non-trivially different, but all have the same order of magnitude. In other words, there are different *local fractal dimensions*. They conclude that the coastline of continental Europe is not *self-similar* but it is *self-affine*. A *self-affine transformation* or an *anisotropic transformation* is a transformation that begins from a point $x = (x_1, ..., x_E)$ in the E-dimension space to arrive in $x\prime = (r_1x_1, ..., r_Ex_E)$ and the factor of scale is not a scalar, but it is a vector $\vec{r} = (r_1, ..., r_E)$. Therefore, in general, a fractal is *self-affine*.

2.2 Introduction to Percolation Theory

2.2.1 The percolation model

The word "*percolation*" is naturally associated with the movement of some fluids through porous media. Until the first half of the 20th century, the scientists studied the percolation phenomena mainly by experiments, due to the difficulty to find exact analytical solutions for most of the problems. After the advent of supercomputers, the computational simulations of physical systems became a very important tool for the scientific community. In 1957, Broadbent and Hammersley published a study [17] that is considered the beginning of the *percolation theory*. In that paper, they defined a model that explained the spread of a fluid or a gas through a random medium [10].

There, we present an introductory example that explain the main concepts of the percolation model and some phenomena associated. Consider a square lattice, initially empty, of dimensions 128×128. We paint some of those squares with black. We also could define a cluster as a group of neighbour squares painted in red in Fig. 2. Therefore, the *percolation theory* deals with the properties of these clusters.

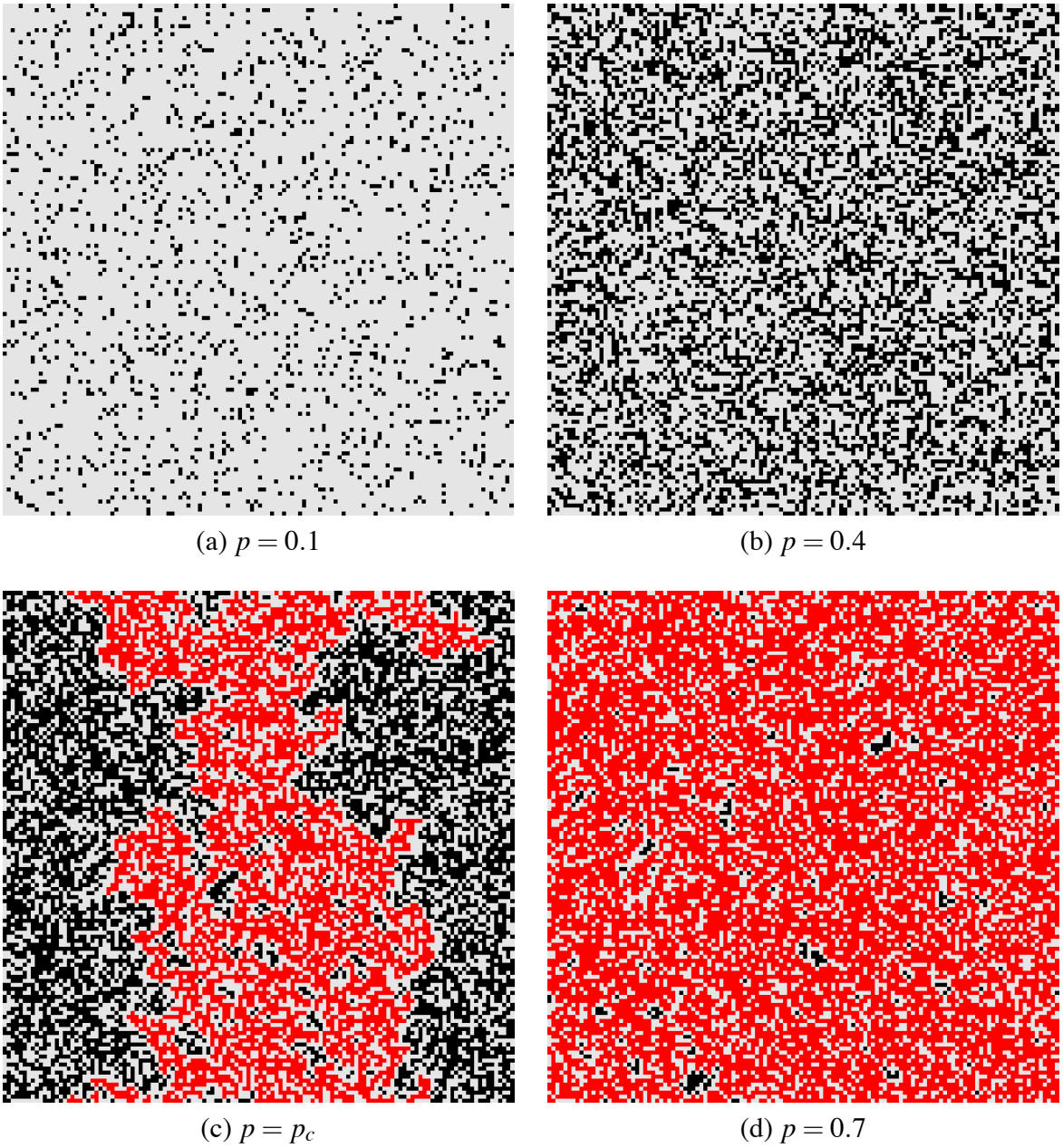

(a) $p = 0.1$ (b) $p = 0.4$

(c) $p = p_c$ (d) $p = 0.7$

Figure 2: The figure shows four square lattice of dimension 128×128 for different values of p. The black squares are the occupied sites and the white squares are the not occupied sites. In red are shown the clusters [18].

Naturally the black squares could be distributed in different ways. We deal with the case where the black squares are distributed randomly. The probability that one square

is black is p, so if we have N squares, where $N \to \infty$, only pN squares are black and $(1-p)N$ squares are empty. From *Introduction to percolation theory* [16], we cite the definition of *percolation theory* given by Stauffer:

> "Each site of a very large lattice is occupied randomly with probability p, independent of its neighbours. Percolation theory deals with the clusters thus formed, in other words with the groups of neighbouring occupied sites."
>
> — Dietrich Stauffer

When the probability reaches $p \geq 0.6$, there is one big cluster that extends from the top to bottom and from left to right of the lattice. When $p = p_c$, the percolation process reveals a second order transition from a locally connected state to a state where the connectivity covers globally network. The phenomena near to the probability p_c are called *critical phenomena* and the theory that deals with these type of problems is the *scaling theory*.

2.2.2 The forest fire model

The *forest fire model* is a simple model of percolation frequently used to study *critical phenomena*. There are two ways to study the propagation of a fire in a forest: One experimental and the other using simulations. Since experimental study is complicated, the simulation is a way to gain some in right on the phenomena. The forest may be simulated using a lattice, exactly as we explained in 2.2.1, however in this case every square is in place. The probability that one square is occupied by a tree with probability p, so the probability that one square is not occupied is $(1-p)$. If $p = 1$ all the squares are occupied and if $p = 0$ there are no trees in the forest. What happens in a natural forest when a fire begins is that the burning trees could burn others that are near them, even though after a period of time the burning tree stops to burn, so it can not burn the others. One can start burning the first bottom row of the lattice. The trees burn for a unit of time and then they stop and disappear. A tree could burn another tree only if this one is a neighbour of the first. We define, as neighbours, only the nearest neighbours of *Von Neumann*, as shown in Fig. 3.

When the probability p is the critical probability p_c, the cluster formed is connected from the bottom to the top. The life time of the fire increases up to p_c and then it decreases, as show in Fig. 4.

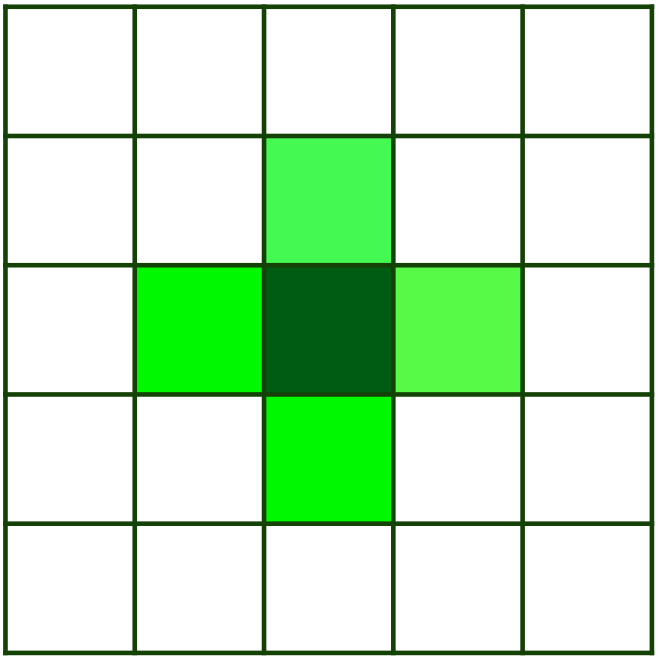

Figure 3: First neighbours of Von Neumann. The dark green represents the tree and in light green are represented the first neighbours of Von Neumann. A tree could burn another tree only if this one is a neighbour of the first.

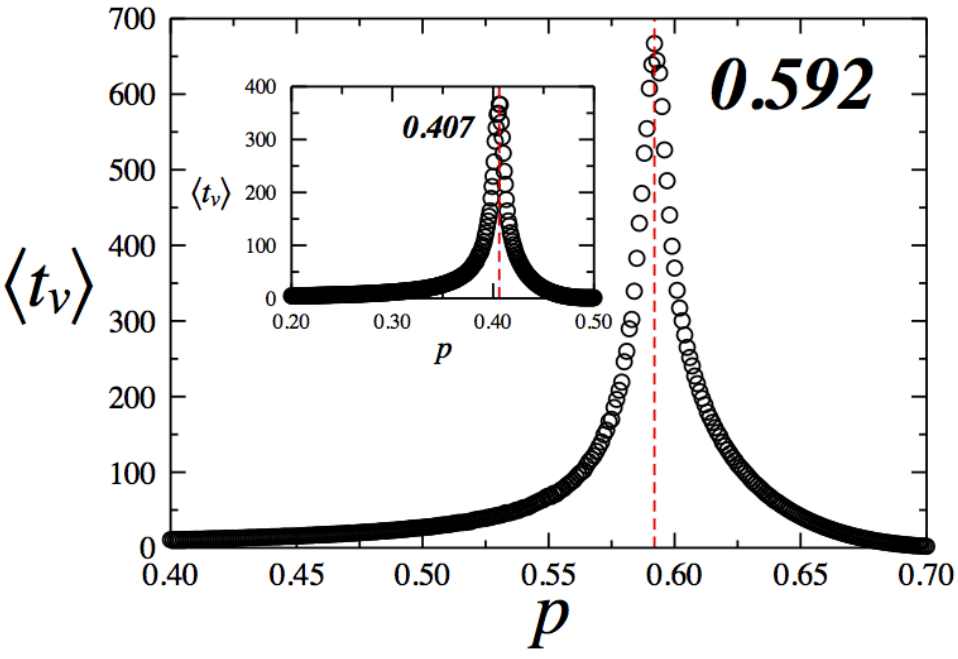

Figure 4: Lifetime $\langle t_v \rangle$ as a function of the probability of occupation for a lattice of size side $L = 1024$ for 1000 samples with Von Neumann neighbours [18].

For $p = 0.592$, we have the maximum of the lifetime $\langle t_v \rangle$ (Fig. 5) [18].

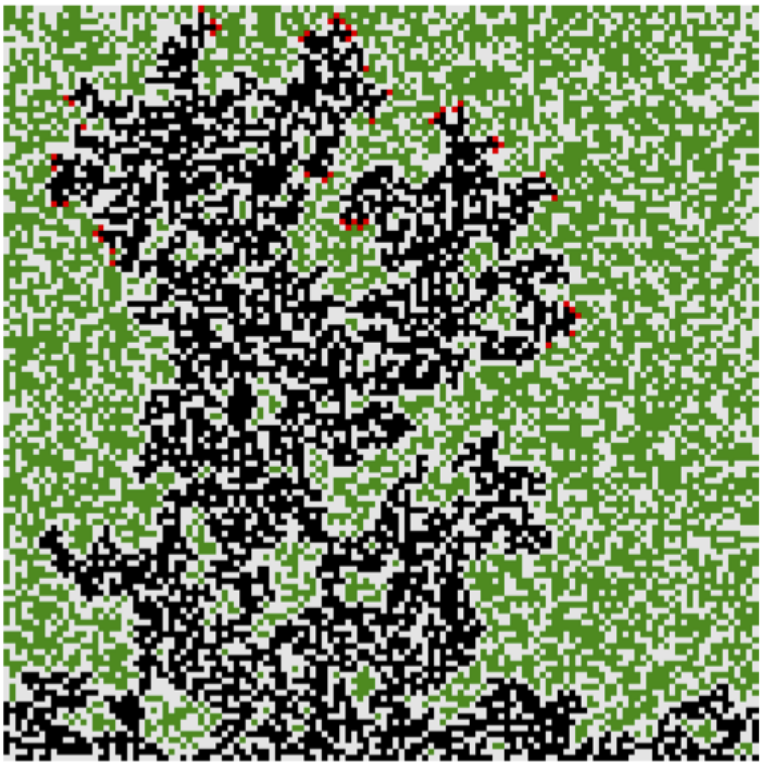

Figure 5: The forest fire model for a lattice of size side $L = 1024$ at $p \cong p_c$. The trees are represented in green, the burning trees in red and the burned trees in black [18].

2.2.3 Percolation theory applied to oil fields

At first sight, it is strange to associate the percolation model with oil field. However if you study the conformation of the rock, its structure is very similar to our lattice previously explained. In this context, it is possible to imagine the white squares as the solid part of the rock and the black squares as the pores where the oil could penetrate. The average concentration of the oil in the rock is the probability of occupation p. The pores are random located with correlations among them and there are some models that allow to simulate this kind of situations [16].

We could start the study of this problem from the most simple case, using the previous structure where the black squares are allocated with a probability p. When working in oil exploration, there is interest in finding large reservoirs of oil that it is represented as a large cluster in our lattice. Therefore, we could understand that if $p < p_c$ the clusters formed are small and if $p > p_c$ the cluster formed is large, so this is the case of interesting. The percolation model can be used in order to simulate a large landscape which it would be impossible to access. One usually considers a small sample of the rocks, normally logs of diameter between 5-10 cm and measure the porosity in this sample. After that, the

structure of the entire rock based on that porosity can be extrapolated. This is a frame of dimension $L \times L$ and it is possible to calculate how many points within this frame are connected with other points. We define the mass $M(L,p)$ as the number of points that belongs to the largest cluster. When $p < p_c$, $M(L,p)$ grows in logarithmic form with the dimension L. When $p > p_c$, we may see that $M(L)$ grows linearly with L^2. When $p \cong p_c$ the situation is different, the cluster possesses a fractal structure that is ramified and many holes are formed within the frame. In this case, $M(L,p)$ grow linearly with L^D, where D is the fractal dimension. $D = 1.9$ in two dimensions. For a three dimensional structure $D = 2.5$. Summarizing,

$$M(L,p) = \begin{cases} ln(L) & if\ p < p_c, \\ L^D & if\ p = p_c, \\ L^d & if\ p > p_c, \end{cases} \tag{2.4}$$

where d is the Euclidean dimension [18]. Numerically, to calculate D we define the gyration radius R as,

$$R^2 = \sum_i \frac{|r_i - r_o|^2}{s}, \tag{2.5}$$

where s is the mass of the big cluster $M(L,p)$, r_i is the position of the i-element and r_o is the position of the center of mass given by,

$$r_o = \sum_i \frac{r_i}{s}. \tag{2.6}$$

Considering the statistics on various samples, in the thermodynamic limit and criticality, we have,

$$M \equiv \langle M(\infty, p_c) \rangle \equiv \langle s \rangle \sim \langle R \rangle^D. \tag{2.7}$$

2.3 Introduction to Graph Theory

2.3.1 The seven bridges of Königsberg

In 1736, the Graph Theory was introduced by Leonhard Euler through the solution of a famous problem, known as the *Seven Bridges of Königsberg* [4] (Fig. 6). Königsberg, actually known as Kaliningrad in Russia, is a city crossed by a river called Pregel. The form of that river produces two islands within the city. These islands are connected with the city by seven bridges.

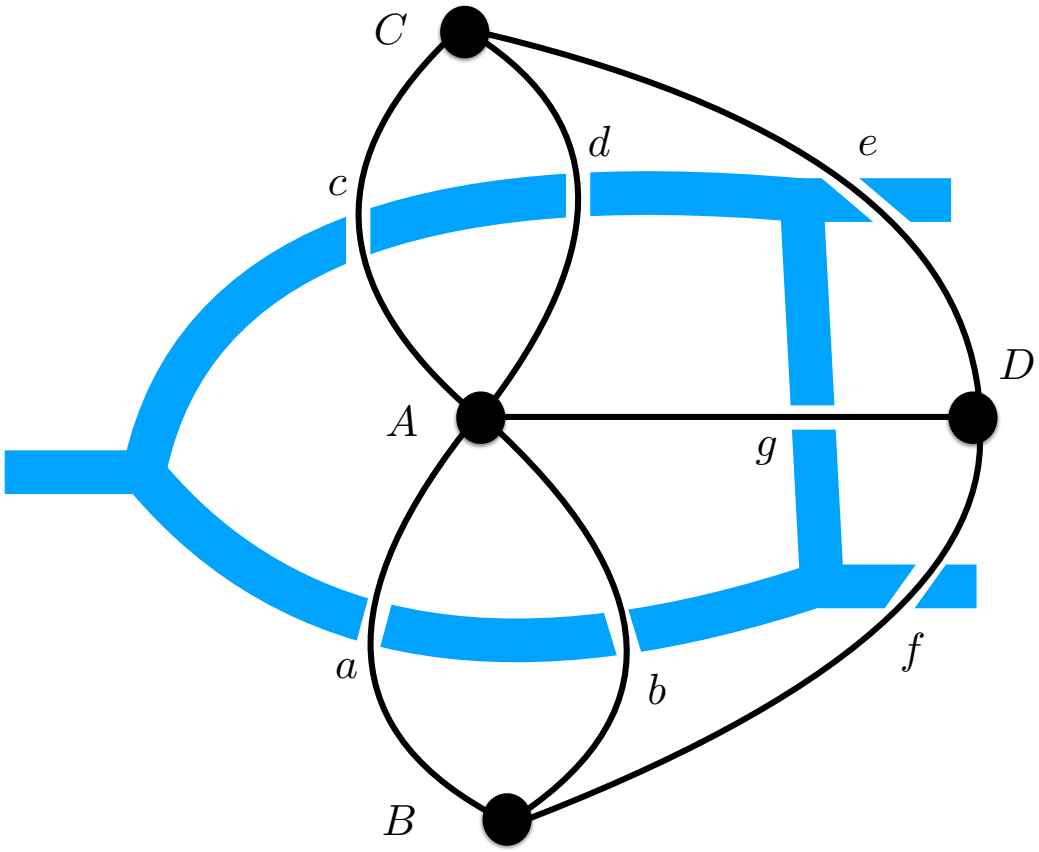

Figure 6: The Seven Bridges of Königsberg. The seven bridges are represented by the letters a, b, c, d, e, f, g and the land is represented by the letters A, B, C, D .

The question was "is it possible to find a path through the city crossing all the bridges once?". The Euler's answer was no, it is not possible. He simplified the problem imagining the land masses as points, called *vertices*, and the bridges as lines that connect the land masses, called *edges*, as shown in Figure 6. Furthermore, the number of edges of each vertex is called *degree*.

It should be noted that from the vertices D, B and C come out three edges and from vertex A comes out five edges. Euler proposed a theorem that explain the viability of a graph, by stating that a graph could be covered if and only if all the vertices have even degrees or if two of the all vertices have odd degrees. However it is necessary to start the navigation from one of these two vertices and finishing in the other one. In Königsberg case, it is impossible to navigate all the graph without passing twice for an edge. In the following years, the graph theory was widely studied and, nowadays, it is a solid field with several application in different areas.

A graph is an ordered pair defined as:

$$G = (V, E), \tag{2.8}$$

where V is the set of vertices and E is the set of edges. The *order* $|V|$ of a graph is the number of vertices in V and the *size* $|E|$ of a graph is the number of edges in E [19]. Another important property is the degree or *valency* $d(v)$ of a vertex v. The degree $d(v)$ is the number of edges that end in that vertex v. If $d(v) = 0$, the vertex is called *isolated* and if $d(v) = 1$, the vertex is called *pendant* or *leaf*. When all the vertices of a graph have the same degree, the graph is called *regular*.

An important graph is the *lattice*, which is a graph that forms a regular tiling. It is drawing embedded in Euclidean space R^n.

2.3.2 Shortest path problem

In order to introduce the concepts related with the *Shortest path problem*, we present the following example. In the end of the day, you want to leave your work place and arrive at home as soon as possible, even though, like you, there are a lot of other people with the same desire. Therefore, you need to find the best route to arrive at your home. In other words, the solution of this important problem is to find the best way from all possible ways. The newest GPS devices estimate the number of cars on the roads and solves this kind of problem for you. The Fig. 7 represents a graph where each vertex is labeled and every edge has a given weight. The shortest path is represented in red. Such path connects the *source* point S and the *target* point F.

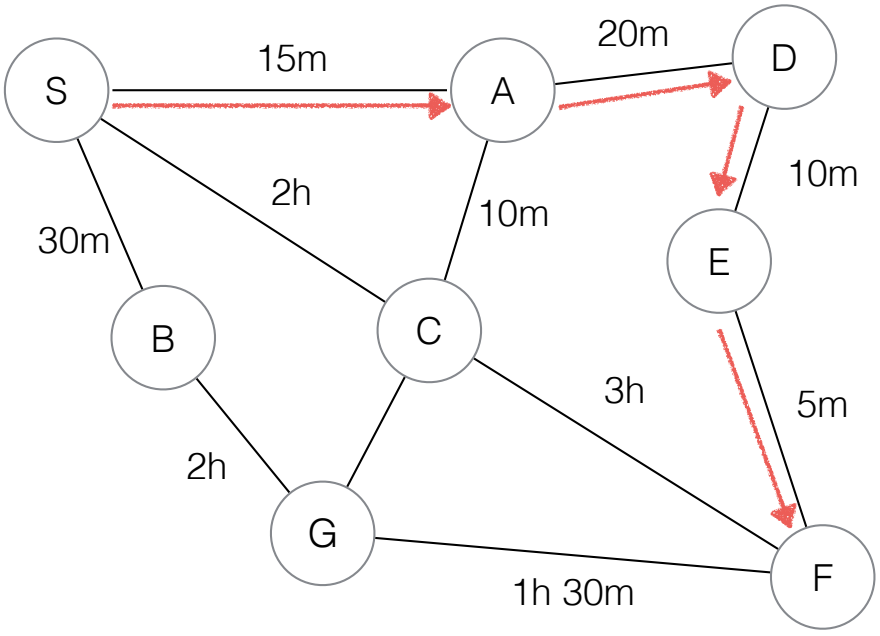

Figure 7: The Figure shows the *shortest path* between the source point S and the target point F. Every vertex is represented by a letter S, A, B, C, D, E, F, G and it is assigned a time value for each edge. The red arrows represent the shortest path.

2.3.3 Optimal path model

In the context of Complex Systems, the shortest path is called the *optimal path* (*OP*) and we could also describe it using the mathematical formalism of the Graph Theory. If we consider a graph,

$$G = (V, E), \tag{2.9}$$

where V is the set of the vertex and E is the set of the edges (u, v), for each edge, we can define a weight function $w(u, v) : E \rightarrow R$. The total weight of the path $p = (v_o, v_1, ..., v_{k-1}, v_k) \in V \times V \times ... \times V$ is the sum of the weight of all the edges in the path,

$$w(p) = w(v_0, v_1, ..., v_{k-1}, v_k) = \sum_{i=1}^{k} w(v_{i-1}, v_i). \tag{2.10}$$

Finally, it is possible to define the weight δ of the shortest path from u and v,

$$\delta(u, v) = \begin{cases} min\{w(p) : u \rightsquigarrow v\} & if\ there\ is\ a\ path \\ \infty & other\ cases \end{cases} \tag{2.11}$$

Therefore, the optimal path between the vertices u and v is defined as any possible path p with weight given by $w(p) = \delta(u, v)$.

2.3.4 Dijkstra's algorithm

The simplest way to solve the optimal path problem, between two nodes of a graph, it is trying all the possible ways and finding the shortest one. However, over the years, several algorithms have been developed to solve this type of problem. The most famous are the *Dijkstra's algorithm* and the *Bellman-Ford's algorithm*. The difference between them is that the Bellman-Ford's algorithm finds the shortest path in a graph with negative and positive weight edges and, in the cad of Dijkstra's algorithm, the weight edges must be positive. Here, we present the Dijkstra's algorithm.

Given the graph $G = (V, E)$, we suppose the existence of two sets: The first set S represents all the vertices that have already an optimal path and the second set $Q = V - S$ represents the vertices that do not have that path yet. For each vertex $v \in V$, we define a "father", the *predecessor* $\pi[v]$. The $\pi[v]$ is the vertex which precedes the vertex v or if the vertex v is the first vertex of a given path, its predecessor is itself. We also define $d[v]$ as the total weight from the source s to v. The algorithm starts from the source s, $d[s] = 0$,

and for all the other vertices, which the shortest path is unknown, we suppose $d[v] = \infty$ $\forall v \neq s$ and $\pi[v] = 0$ $\forall v \in V$. At this moment, we have $Q = V$, therefore $S = \{0\}$. Proceeding with the rest of the algorithm, we extract the vertex of minimum weight u in Q, put it in the set S and calculate the total weight from the source s to all neighbours of u. If the weight calculated is lower than the weight previously calculated, we update the weight and the predecessor of that vertex. This procedure is called *relaxation technique*. After that, we restart the process: We find the minimum from the Q set, put it in the S set and continue the algorithm as before. The algorithm concludes when $Q = \{0\}$, in other words, when all shortest path have been found. We show an example of the Dijkstra's algorithm in Fig. 8 [18][20][21].

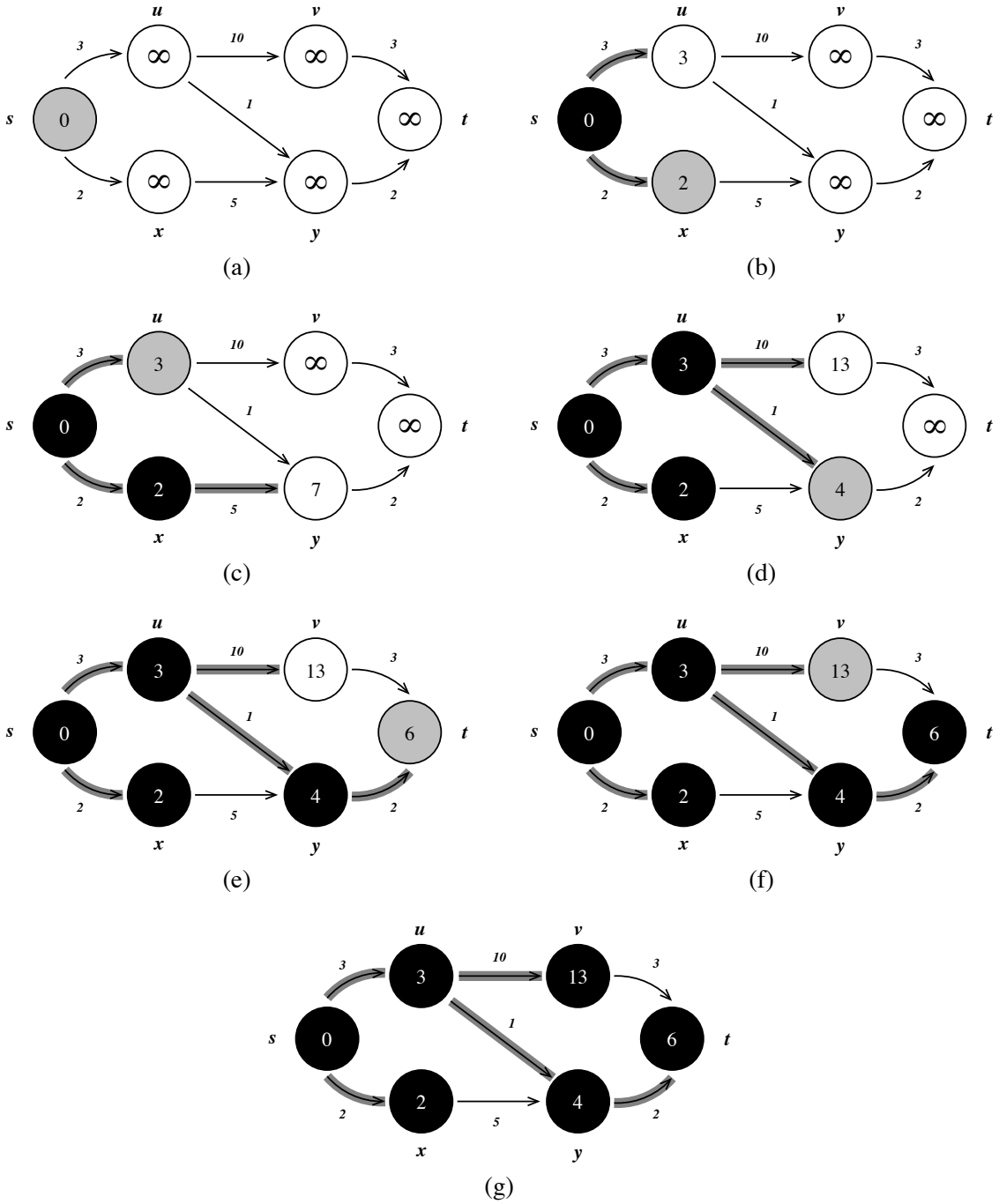

Figure 8: Example of an application of the Dijkstra's algorithm step by step [18]. The black vertices belongs to the S set. The shaded vertices are those that have the minimum value within the Q set, where $Q = V - S$. The shaded edges represent the connections with the predecessors. The algorithm will find all the shortest path among the source vertex and all the other vertices [18].

3 DYNAMIC TIME WARPING AND INTERPOLATION TECHNIQUES

3.1 Dynamic Time Warping

In 1978, H. Sakoe and S. Chiba introduced the *Dynamic Time Warping* (DTW) in a study about spoken word recognition [23]. The DTW allow us to relate two temporal sequences with an non-trivial correlation between them by the introduction of a lattice problem. Precisely, DTW can be used when a sequence correspond to a distortion of the other or to automatically cope with time and speed deformations associated with time-dependent data [22]. Considering two time-dependent correlated sequence, $X = \{x_1, x_2, ..., x_N\}$ and $Y = \{y_1, y_2, ..., y_M\}$, where $N, M \in \mathbb{N}$. The aim of this algorithm is to find a relation between these sequences through alignment, as shown in Fig. 9.

We first define a *feature space* F, where $x_n, y_m \in F$ for $n \in [1:N]$ and $m \in [1:M]$. In order to compare these sequences, we define a *local cost measure* $c(x, y)$, such that $c : F \times F \to \mathbb{R} \geq 0$. If $c(x, y)$ is small (low cost), x and y are similar, and if $c(x, y)$ is large (high cost), x and y are not similar.

Taking into account all the possible pairs of elements, we define the *cost matrix*,

$$C(n, m) = c(x_n, y_m), \tag{3.1}$$

where $C \in \mathbb{R}^{N \times M}$. After that, the aim is to find a path in the matrix to depict the correlations among the elements of each sequence.

Following [22], *a (N, M)-warping path, or simply warping path, is a sequence $p = (p_1, ..., p_L)$ with $p_l = (n_l, m_l) \in [1:N] \times [1:M]$ for $l \in [1:L]$ satisfying the following three conditions*:

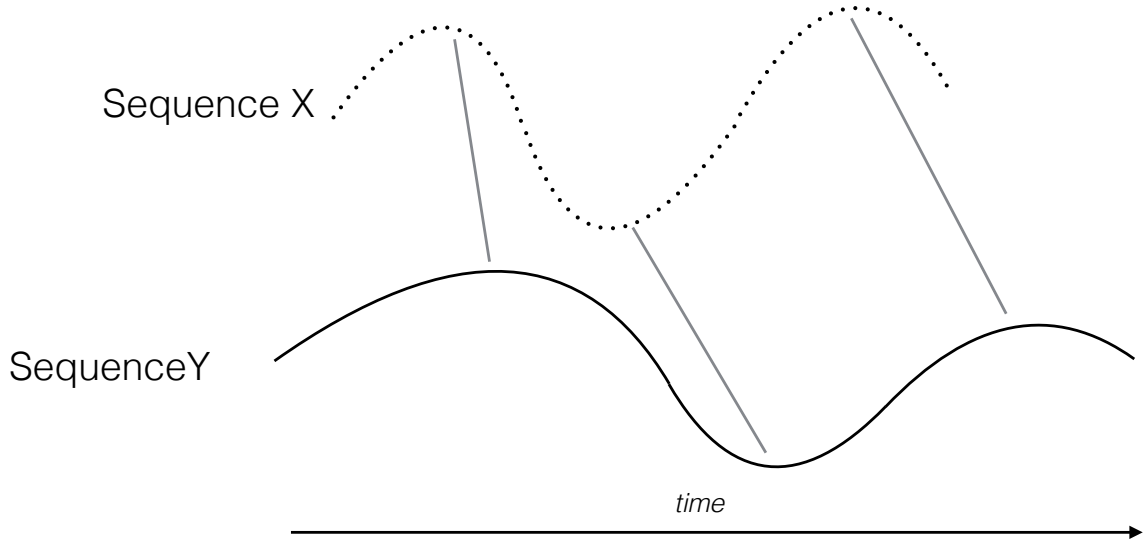

Figure 9: Alignment of two time-dependent sequences $X(t) = \{x_{t_1}, x_{t_2}, ..., x_{t_N}\}$ and $Y(t) = \{y_{t_1}, y_{t_2}, ..., y_{t_M}\}$, where $N, M \in \mathbb{N}$. The grey lines represent the correlations between the series.

1. Boundary condition: $p_1 = (1, 1)$ and $p_L = (N, M)$;
2. Monotonicity condition: $n_1 \geq n_2 \geq ... \geq n_L$ and $m_1 \geq m_2 \geq ... \geq m_L$;
3. Step size condition: $p_{l+1} - p_l \in \{(1, 0), (0, 1), (1, 1)\}$ for $l \in [1 : L - 1]$.

The boundary condition imposes the correlations between the sequences. In fact, the first and the last element of each sequence are correlated with themselves. Furthermore, the monotonicity condition implies that the order of the elements in a sequence is the same in the another sequence and the step size condition is a continuity condition. Therefore, there are not replications in the alignment. We define the *total cost* $c_p(X, Y)$ of the warping path p between X and Y as:

$$c_p(X, Y) = \sum_{l=1}^{L} c(x_{nl}, y_{ml}). \tag{3.2}$$

Up to this point, we defined the general characteristics of the path. However, a lot of paths obey the conditions previous listed. The *optimal warping path* p^* is the path, among all the existing paths, that has the minimal total cost. The *DTW distance* DTW(X,Y) between X and Y is the cost of p^*,

$$DTW(X, Y) = c_{p^*}(X, Y) = min\{c_p(X, Y) \mid p\ is\ an\ (N, M) - warping\ path\} \tag{3.3}$$

The DTW distance is well-defined if there are not several shortest paths. It is symmetric if the local cost measure c is symmetric. Once we find the optimal warping path, we have the evidence of correlation between the sequences.

3.2 Interpolation with DTW

3.2.1 Dynamic Time Warping Interpolation (DTWI)

As we already introduced in this chapter, H. Sakoe and S. Chiba defined a model called *Dynamic Time Warping* DTW [23] for the local detection of similarity between two time-dependent sequences. We developed the Dynamic Time Warping Interpolation DTWI, an interpolation strategy based on DTW. Considering two time-dependent sequence, $X = \{x_1, x_2, ..., x_N\}$ and $Y = \{y_1, y_2, ..., y_N\}$, where $N \in \mathbb{N}$, placed with a distance d between them. In Fig. 10 is shown an example where the two sequences are two gaussian. The result of a standard linear interpolation SLI, with the purpose to interpolate a sequence in the middle of the two, is shown in Fig. 11. The black arrow in the Fig. 11 shows that the SLI take into account the vertical correlations between the two sequences, the time grows in the vertical direction. Instead, a DTWI strategy starts from the construction of the

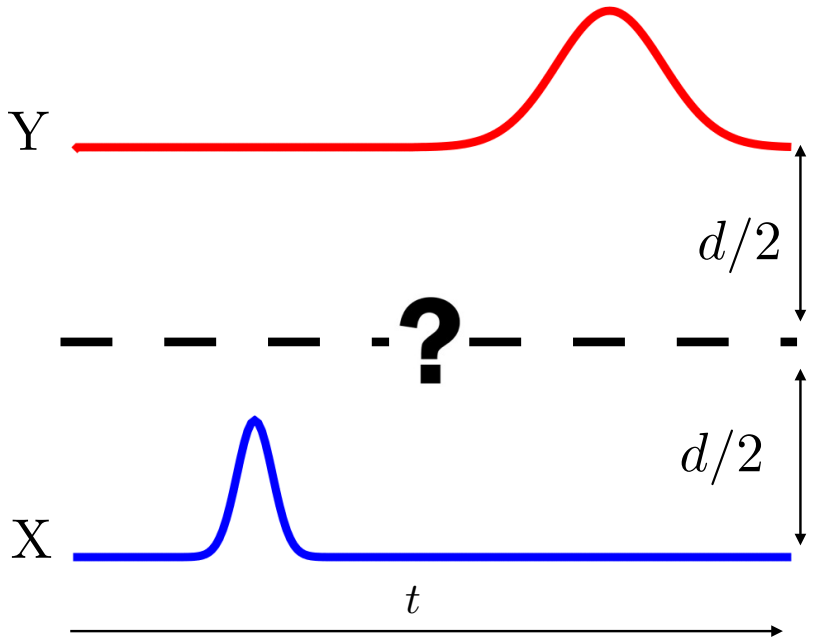

Figure 10: Two time-dependent gaussian sequences $X = \{x_1, x_2, ..., x_N\}$ in blue and $Y = \{y_1, y_2, ..., y_N\}$ in red, where $N \in \mathbb{N}$, separated by a distance d. The dashed black line represents the unknown sequence to interpolate.

cost matrix $C(i, j) = c(x_i, y_j)$ where $x_i, y_j \in F$ for $i, j \in [1 : N]$. Then, we find an optimal

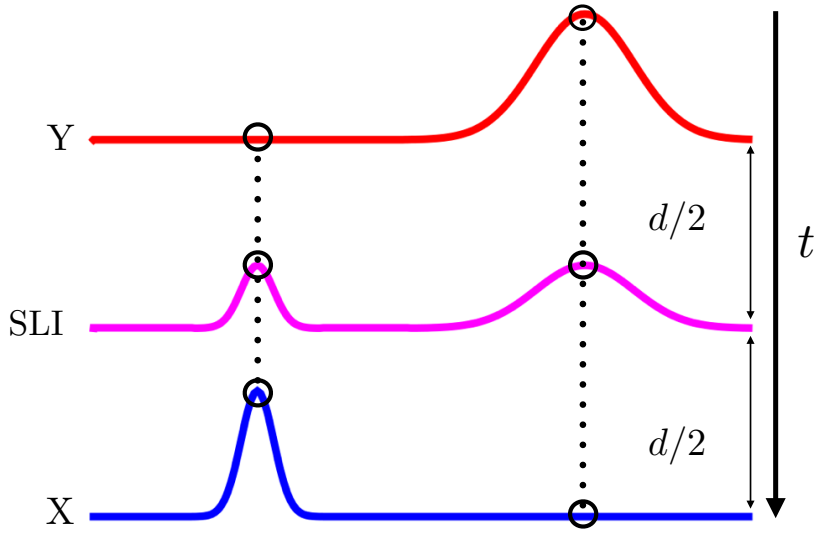

Figure 11: Standard Linear Interpolation (SLI) between two time-dependent gaussian sequences $X = \{x_1, x_2, ..., x_N\}$ in blue and $Y = \{y_1, y_2, ..., y_N\}$ in red, where $N \in \mathbb{N}$, separated by a distance d. The pink sequence represents the result of the SLI where the interpolated sequence is in the middle of X and Y. A SLI provides an interpolation where the time flows from top to bottom or vice versa.

warping path OWP, observing the *Boundary condition*, the *Monotonicity condition* and the *Step size condition* as explained in the previous section. The cost matrix and the OWP is shown in Fig. 12. A linear interpolation among the coordinates indicated by the OWP of the cost matrix, allow us to interpolate the sequence in the middle. The DTWI takes into account the horizontal correlation between the sequences, the time grows in the horizontal direction as shown in Fig. 13.

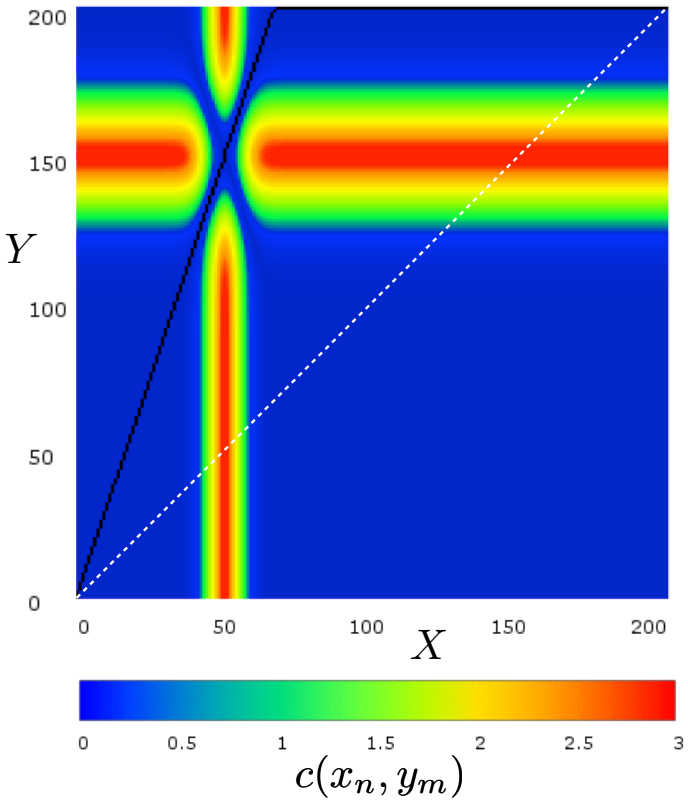

Figure 12: The figure shows the cost matrix generated starting from the two sequences X and Y. Each site is defined by $C(i,j) = |x_i - y_j|$ and the colour scale represents the level of correlations between the two points x_i and y_j of the sequences. Blue represents an high correlation and red a low correlation.The black path represents the Optimal Warping Path (OWP).

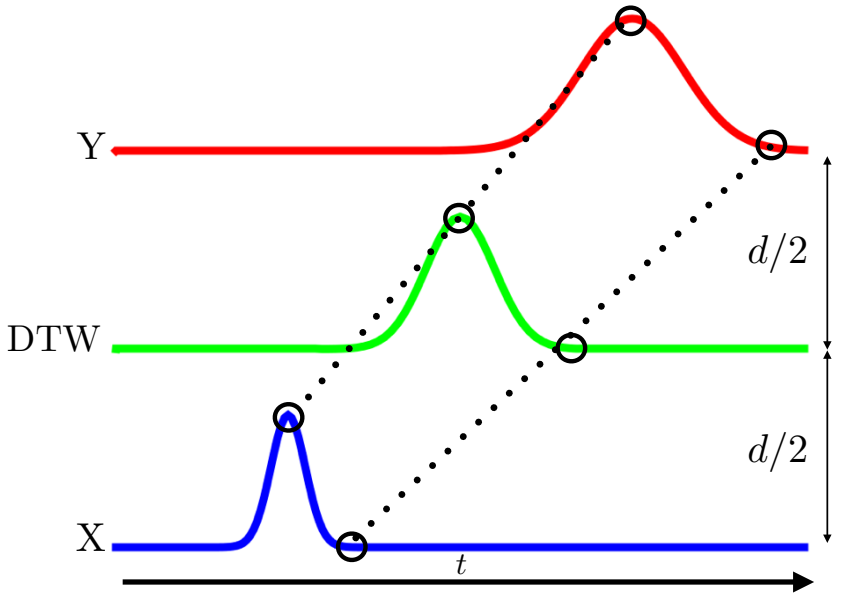

Figure 13: Dynamic Time Warping Interpolation (DTWI) between two time-dependent gaussian sequences $X = \{x_1, x_2, ..., x_N\}$ in blue and $Y = \{y_1, y_2, ..., y_N\}$ in red, where $N \in \mathbb{N}$, separated by a distance d. The green sequence represents the result of the DTWI where the interpolated sequence is in the middle of X and Y. A DTWI provides an interpolation where the time flows from right to left or vice versa.

3.2.2 Where is the oil?

In the modern world, our lifestyle depends on the energy. Actually, we live using an expressive quantity of energy daily wherever we are. This lifestyle began during the industrial revolution by the massive exploration of the fossil fuels.

In the oil industry, it is essential to have the knowledge of the lithology of stratified rocks. Therefore, the challenge is to know where are placed the oil and natural gases reservoirs in order to drill the soil efficiently and consequently obtain an economical profit. In this context, the predictions of earth profiles through reflection of mechanical waves in the soil and the resulting analysis of seismological data is highly relevant for the extraction of such hydrocarbons. The image of the seismic mapping due to wave refraction and reflection into the soil could be analysed to find geological formations of interest.In particular, we deal with the case that we want to reconstruct some depth profiles based on others.

3.2.3 Interpolation strategy

We apply the DTW model, previously used only to analyse the correlations between two sequences, to build an interpolation strategy in order to recover the data of a given earth region. Thereby, we start from two depth profiles $f_1(i)$ and $f_2(j)$, where $i, j = \{1, 2, ..., N\}$, as shown in Fig. 15a and 15b from the landscape in Fig 14. In few words, these sequences represent a characteristic of the earth in function of the depth. The idea is to apply the *Dynamic Time Warping Interpolation* (DTWI) to these sequences, once we know they are correlated with each other. As we stated, the DTW technique deals with *spoken word recognition* or other type of sequences and the DTW potentiality consists in the analysis of distorted signals. Thereby, are we sure the depth-dependent sequences behave as distorted signals? The answer is not, necessarily this case is not that simple. The stratigraphy of the earth is not a simple field, however the innovation of our study lies here. Allied with the DTWI strategy of two depth-dependent sequences, we use this interpolation strategy in order to find the others depth-dependent profiles.

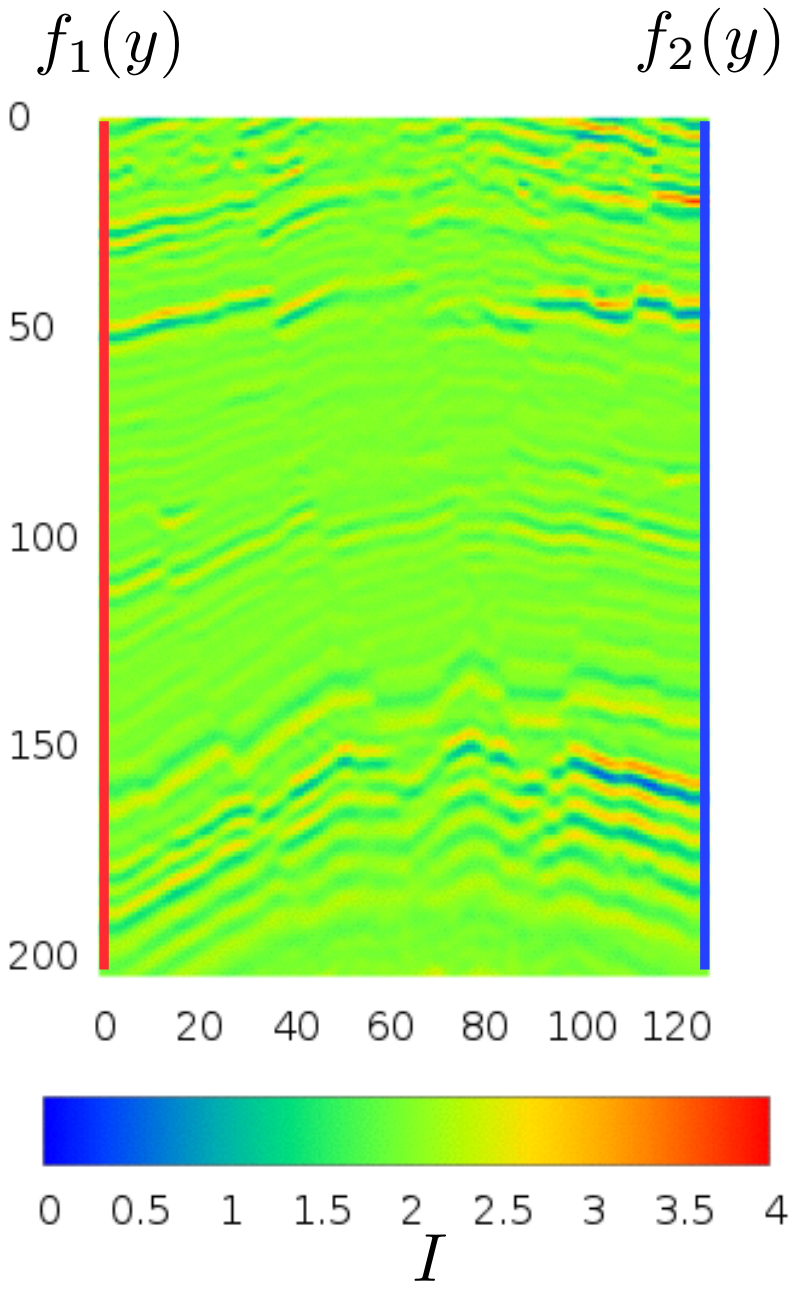

Figure 14: Seismic data provided from WesternGeco [24]. The landscape is formed by 129 sequences made by 201 points each one. The colour scale represents the variation of a characteristic of the soil. The red line represents $f_1(y)$ and the blue line $f_2(y)$. I is the intensity of the seismic signal.

Initially, we use the two father sequences to build the *cost matrix*, where each site is $c(i,j) = |f_1(i) - f_2(j)|$. The $c(i,j)$ is small when the elements of the two sequences are similar and $c(i,j)$ is large when the elements of the two sequences are different (Fig. 16).

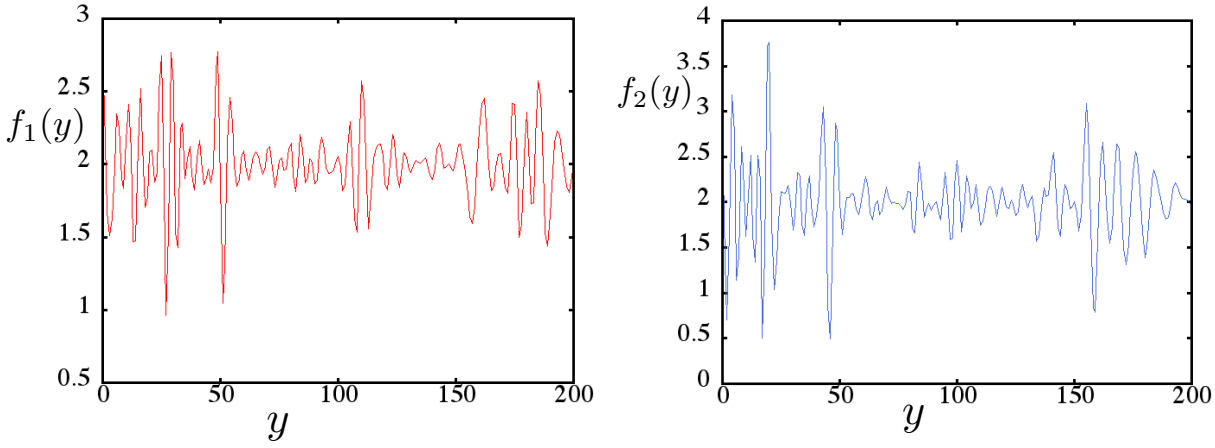

(a) f_1 (b) f_2

Figure 15: Sequences depth-dependent $f_1(y)$ in Fig. 15a and $f_2(y)$ in Fig. 15b. The y represents the depth and $f_1(y)$ and $f_2(y)$ represent a characteristic of the earth in function of the depth.

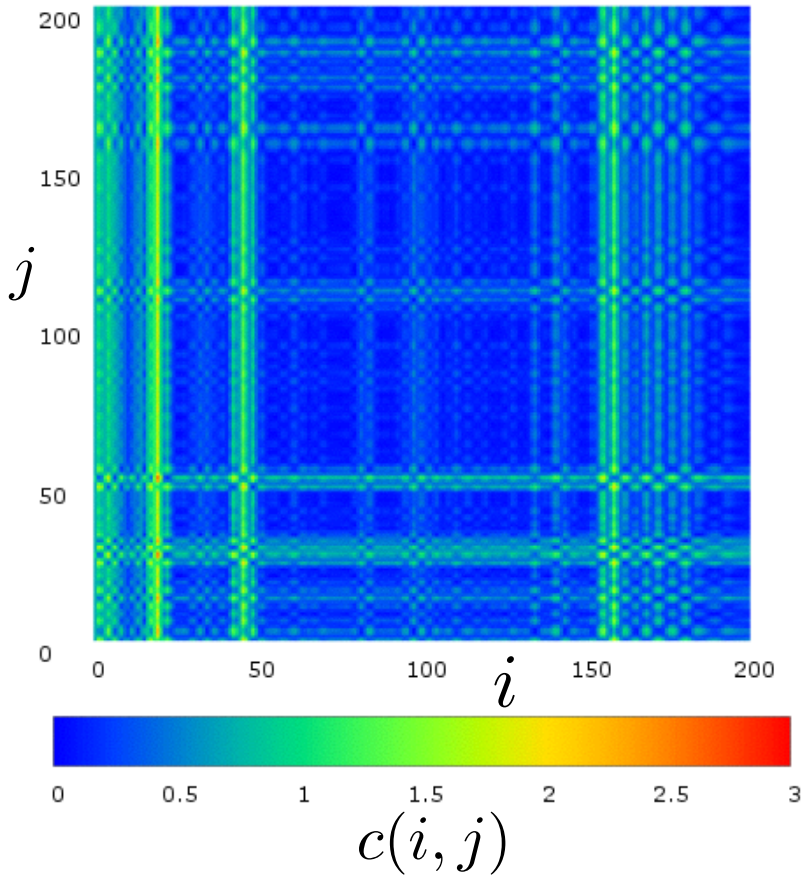

Figure 16: An example of the *cost matrix* generated by using the two sequences $f_1(y)$ and $f_2(y)$ showed in Fig. 15a and 15b. The weight of each site is given by $c(i,j) = |f_1(i) - f_2(j)|$, where $i, j = \{1, 2, ..., N\}$. The colour scale vary from blue (high correlation) to red (low correlation).

After building the *cost matrix*, we have to find the warping path that allow us to show the correlations between the sequences. There are a lot of possible paths in this landscape, however the aim is to find the optimal warping path, the warping path with minimized total weight. Therefore, this path must be the *shortest path* between the points $(1,1)$ and (N,N), where N is the dimension of each sequence.The optimal warping path is defined as follows:

$$p_k = c_k(i_k, j_k) \quad k \in [1:L]\,, \tag{3.4}$$

where L is the length of the path whose weight is given by,

$$w(p) = min\left\{\sum_{i=1}^{L} p_i : (1,1) \rightsquigarrow (N,N)\right\}. \tag{3.5}$$

Furthermore, we have imposed the following conditions:

1. Boundary condition: $p_{initial} = (1,1)$ and $p_{final} = (N,N)$.
2. Monotonicity condition: $i_1 \geq i_2 \geq ... \geq i_L$ and $j_1 \geq j_2 \geq ... \geq j_L$.
3. Step size condition: $p_{l+1} - p_l \in \{(1,0),(0,1),(1,1)\}$ for $l \in [1:L-1]$ where $l \in [1:L]$.

The second and third conditions imply which direction the path could take. Each point of the matrix is therefore "connected" only with three other points (Fig. 17).

As discussed in the previous chapter, there are several algorithms that allow us to find the shortest path. Here we use the *Dijkstra's algorithm*, which only riquires the condition that each site must have a positive weight, and, in our case, each site is positive due to the structure of the cost matrix. One should notice that, in our case the weights are not in the edges but in the sites. This change does not create any problem since the only difference is that the weight will be counted whenever it passes through a site and not when it crosses an edge. With these conditions, it is possible to find the *optimal warping path*, as shown in Fig. 18.

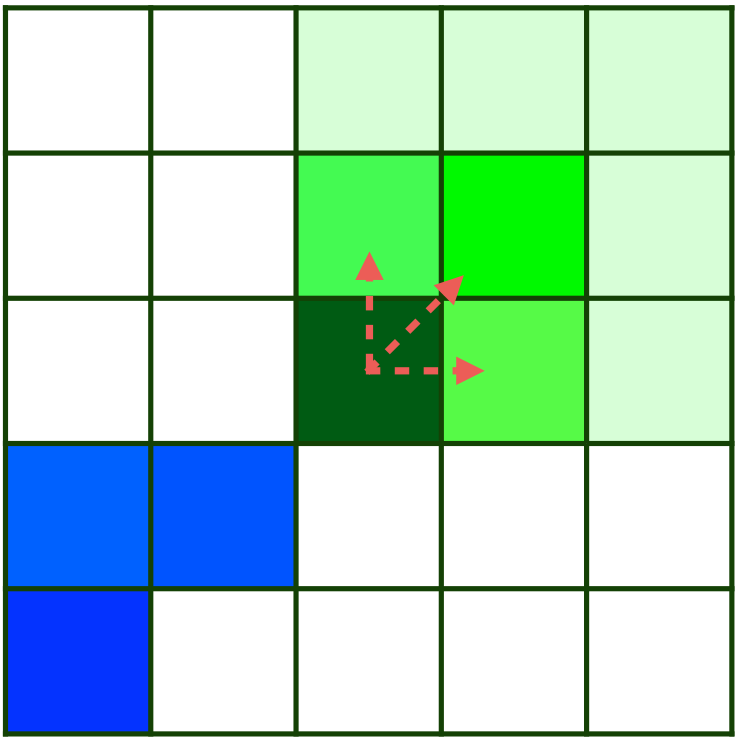

Figure 17: The second and the third conditions imply that the path at a given site could take three directions only. In order to develop the path, the blue squares represent the predecessors of the dark green square. From the dark green square, the path may follow only one of the three directions marked by the red dashed arrows. The possible next site of the path can be only one of the squares painted by light green.

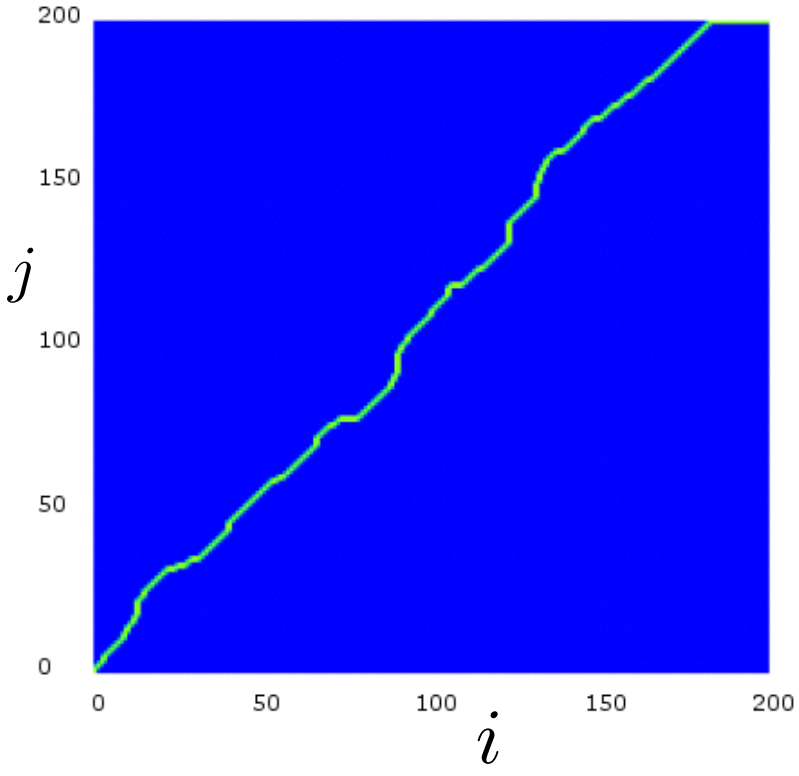

Figure 18: In green the optimal warping path p_k resulting from the cost matrix of the Fig. 16, where the sequences used are $f_1(y)$ and $f_2(y)$. In light blue, the external points of the path.

Each point $p_k = (i_k, j_k)$ of the *optimal warping path* represents a correlation between the two sequences. They are coordinated, so we can identify which point of one sequence is correlated with a point of the other sequence. We are simply following the DTW method with two sequences that derive from seismic data. Precisely, they are two depth-dependent sequences of the landscape in Fig. 14, precisely they are the first and the last sequence.The innovation is here: we use the pieces of information obtained from the DTW to interpolate the space between the sequences. The Figure 19 shows a schematic representation of this strategy. However, there are a lot of other sequences we want to simulate between the red and the blue sequences, precisely 127 that we assume to be unknown.

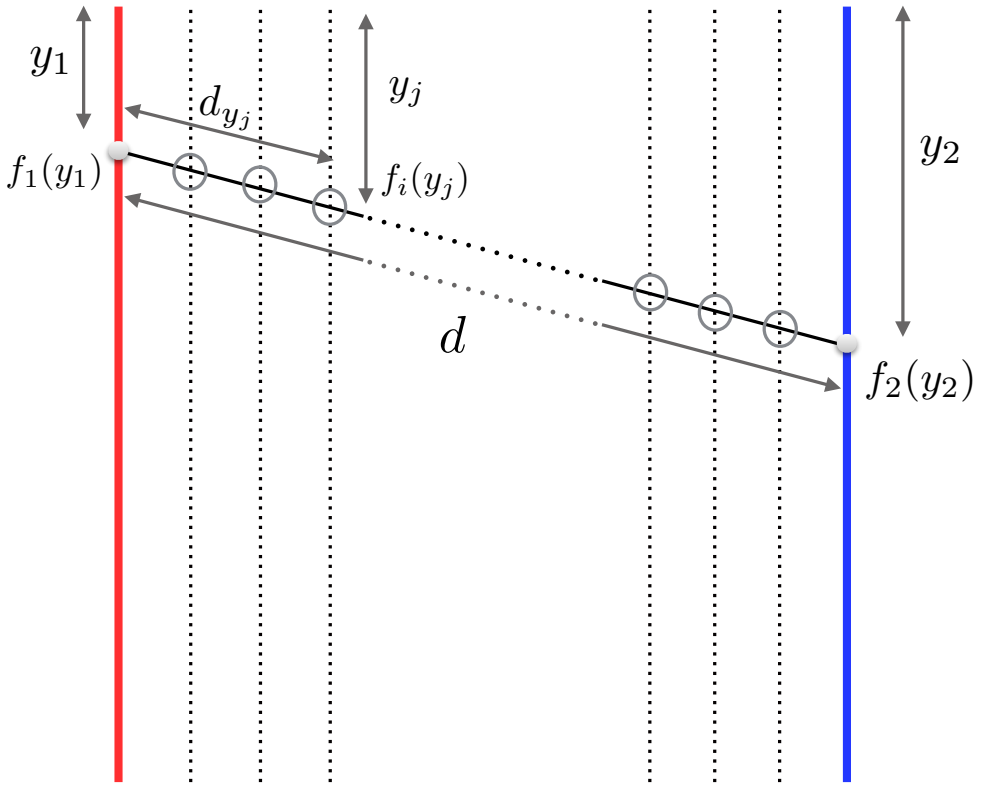

Figure 19: Linear Interpolation between two points of the sequences $f_1(y)$ and $f_2(y)$ using DTWI. $f_1(y_1)$ and $f_2(y_2)$ are the two elements of the sequences that are correlated, where y_1 and y_2 are the respective depths. This result comes from the optimal warping path. d is the distance between the two points of the sequences. d_{y_j} is the distance of the interpolated point $f_i(y_j)$ from the point $f_1(y_1)$, and y_j is its depth.

In order to interpolate the values of the sequences between the two considered sequences, we use a simple linear interpolation,

$$f_i(y_j) = f_1(y_1) + \frac{f_2(y_2) - f_1(y_1)}{d} d_{y_j}, \tag{3.6}$$

where $i \in [1, 129]$ and y_j is the depth of the interpolated point. Applying this interpolation strategy for all the points of the sequence, we obtain a simulation of the full landscape as shown in Fig. 20.

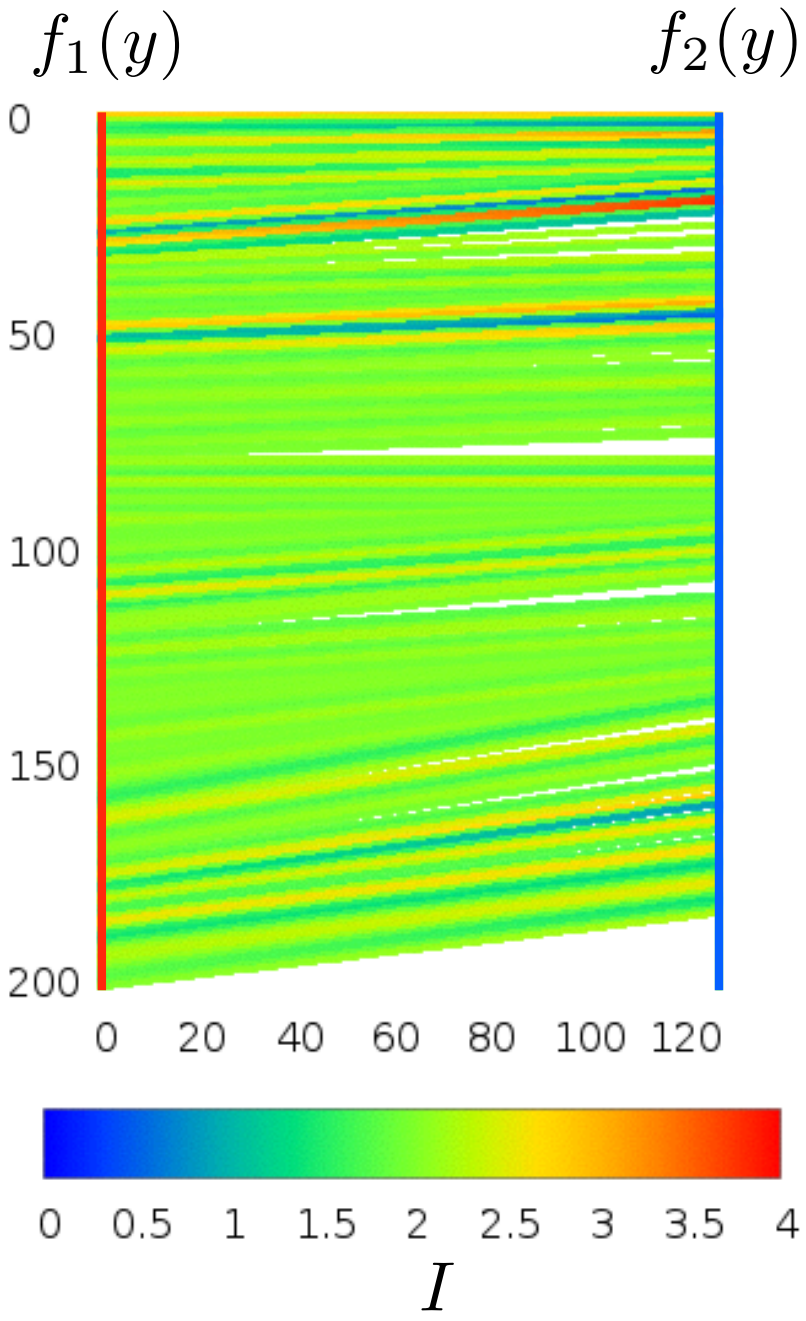

Figure 20: Interpolated landscape from seismic data using only the two series $f_1(y)$ and $f_2(y)$ presented in Fig. 15a and 15b with DTWI.

In particular, Fig. 20 shows the landscape simulated using the first and the last sequence. The results are not good, because the distance between the sequences is very large, making the sequences almost uncorrelated. In order to test our method, we divide the landscape

in much smaller landscapes. After that, we compare our results with the real data and with the result of a *standard linear interpolation* (SLI) to verify that our technique is better than the standard. As shown in Fig. 21, a *standard linear interpolation* is merely a linear interpolation between the points with same depth-level in the two sequences,

$$f_i(y) = f_1(y) + \frac{f_2(y) - f_1(y)}{d} d_i, \tag{3.7}$$

where $f_i(y)$ is the intensity of the interpolated point and d_i is the distance between the first known sequence and the simulated point.

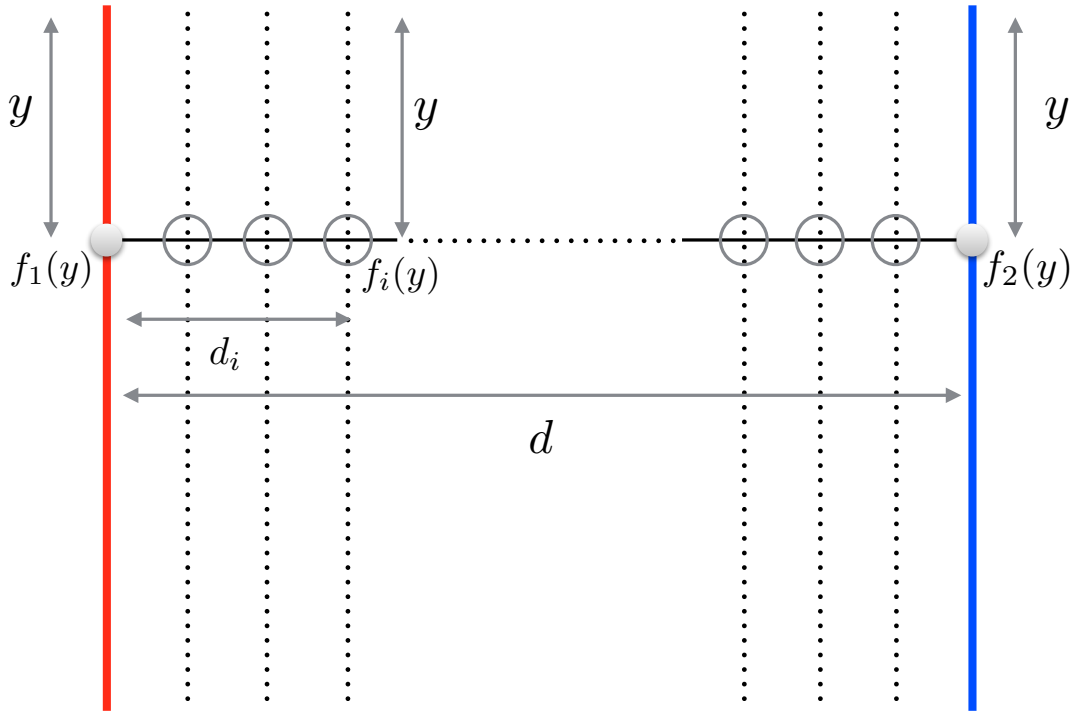

Figure 21: Linear Interpolation between two points of the sequences $f_1(y)$ and $f_2(y)$ using SLI technique. The $f_1(y)$ and $f_2(y)$ are two values of the known sequences at the same depth y. $f_i(y)$ is the interpolated point, where d is the distance between the known sequences and d_i is the distance between the first known sequence and the simulated point.

3.3 Results

In this section, we present the results of our study. We start from a landscape given by WesternGeco [24] of a seismic profile (Fig. 14). The different colours in the Fig. 14 are

due to the stratigraphy nature of the earth. During the years the different layers of rocks settled one above the other, forming the classic stratigraphy conformation. This implies that we can find different types of rocks, at the same depth, depending on the region. We have started applying the DTWI for the first and the last sequence of landscape. After that, we divided the landscape in two and applied the same technique in each new landscape. Actually, we continued this process until only one sequence to interpolate remains. Initially, we consider that only two sequences are known from the real landscape. After that, three sequences used. In the third five sequences, and so forth. Therefore, the number of known sequences is,

$$m = 2^{\mu} + 1 \quad \mu \in [0:6]. \tag{3.8}$$

For each m, we perform an interpolation for the entire landscape. The interval of m depends on the number of sequences of the real landscape. The maximum value of m represents a situation where between the two known sequences there is only one unknown sequence. The results, for the different values of m, are presented in Fig. 22. Next, we simulated the same landscape, however using the SLI, as explained in the previous section. The results are shown in Fig. 23.

We presented the simulated landscapes obtained by using the DTWI and by using SLI for each value of m. As shown in Fig. 19, the depth of the points interpolated by the DTWI do not coincide necessarily with the depth of the real points, because the interpolation is made by two points of different depths. The difference between the depths could create area where we can not have information as shown in Fig. 22. In order to compare the results of DTWI and SLI, we calculate the square error for the DTWI case and for the SLI case. For the SLI case, as the points interpolated are at the same depth of the real data, as shown in Fig. 21, we calculated the square error in these points. For the DTWI case, as the depth of the points interpolated by the DTWI do not coincide necessarily with the depth of the real points, before we interpolate the real data using a linear interpolation to find the points interpolated by the DTWI. The *square error* Err^2_{DTWI} is calculated as follows:,

$$Err^2_{DTWI} = \frac{\sum_{i=1}^{N}[f_{DTWI}(i) - f_{real_{interpolated}}(i)]^2}{N}. \tag{3.9}$$

Using the SLI, the *square error* Err^2_{SLI} is calculated as following,

$$Err^2_{SLI} = \frac{\sum_{i=1}^{N}[f_{SLI}(i) - f_{real}(i)]^2}{N}, \tag{3.10}$$

where the sets of $f_{DTWI}(i)$ and $f_{SLI}(i)$ represents the points interpolated by the two

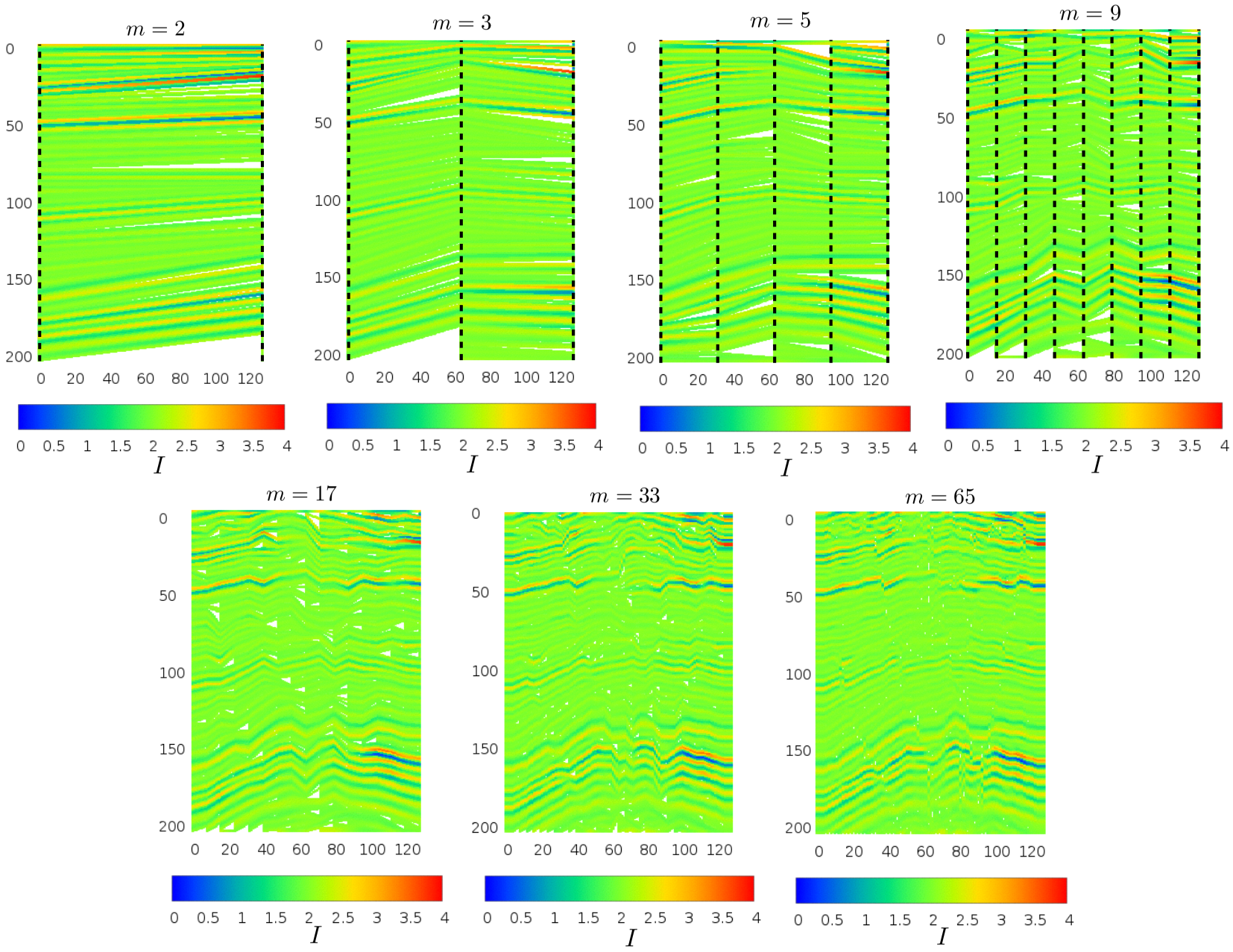

Figure 22: DTWI applied to interpolate the lithology of the stratified rocks, starting from a real landscape (Fig. 14). The m value represents the number of known sequences, $m = \{2, 3, 5, 9, 17, 33, 65\}$. Each figure represents the interpolated landscape with a different value of m. I is the intensity of the seismic signal. The dashed black lines represent the known sequences when $m = 2, 3, 5, 9$. When $m = 17, 33, 65$ there are not dashed black lines because the distance among them is too small to be represented.

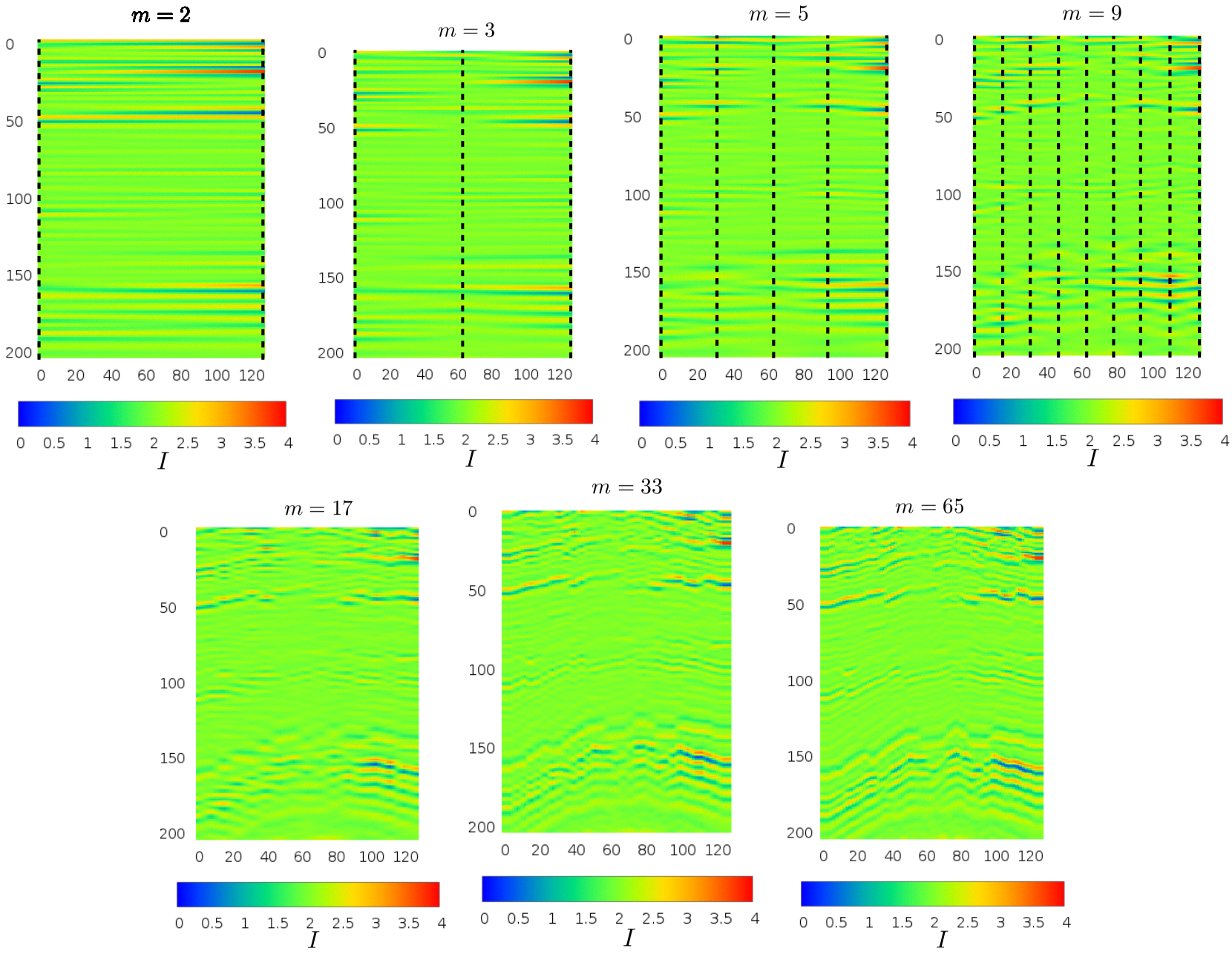

Figure 23: SLI technique applied to interpolate the lithology of the stratified rocks, starting from a real landscape (Fig. 14). The m value represents the number of known sequences, $m = \{2, 3, 5, 9, 17, 33, 65\}$. Each figure represents the interpolated landscape with a different value of m. I is the intensity of the seismic signal. The dashed black lines represent the known sequences when $m = 2, 3, 5, 9$. When $m = 17, 33, 65$ there are not dashed black lines because the distance among them is too small to be represented.

techniques. $f_{real}(i)$ is the set of real data and $f_{real_{interpolated}}(i)$ is the set of real data interpolated to find the points at the same depth of the points interpolated with the DTWI. N is the numbers of the interpolated points. The result of this comparison is presented in Fig. 24.

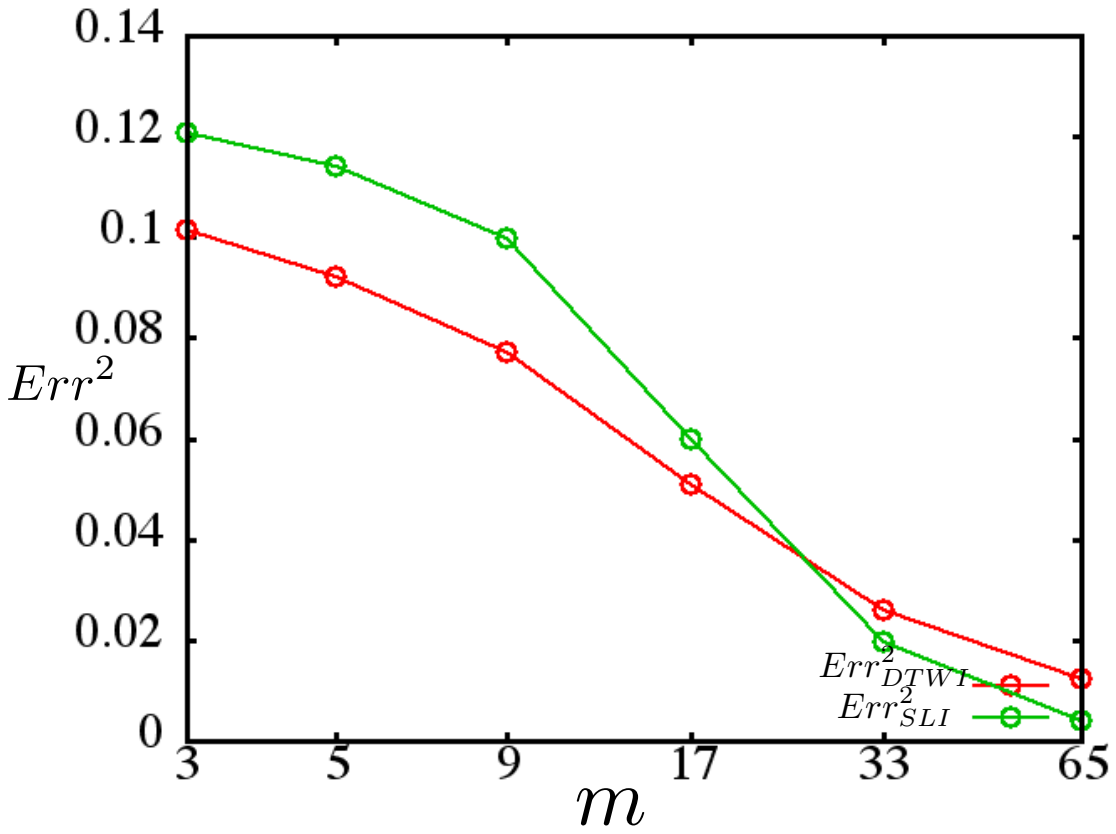

Figure 24: The graph represents the *square error* Err^2 for the DTWI interpolation strategy Err^2_{DTWI} in red and for the SLI techniques Err^2_{SLI} in green in function of the number of known sequences m in a logarithmic scale. For $m = 3, 5, 9, 17$ the Err^2_{DTWI} is less than the Err^2_{SLI}.

The Figure 24 shows that the DTWI is better than the SLI technique when sequences $3, 5, 9, 17$ are known. When $m = 9$ the Err^2_{DTWI} is much lower then Err^2_{SLI}, with a percentage difference of $\sim 30\%$, as shown in Fig. 25. The Fig. 25 shows the evolution of the percentage difference,

$$\%Diff_{DTWI,SLI} = \frac{Err^2_{SLI} - Err^2_{DTWI}}{Err^2_{DTWI}} 100, \tag{3.11}$$

in function of the number of known sequences m. Comparing the real landscape and the landscape interpolated using the DTWI when $m = 9$, we conjecture that the DTWI works better when the horizontal pattern of the soil has the same order size of the distance between the sequences considered in the DTWI.

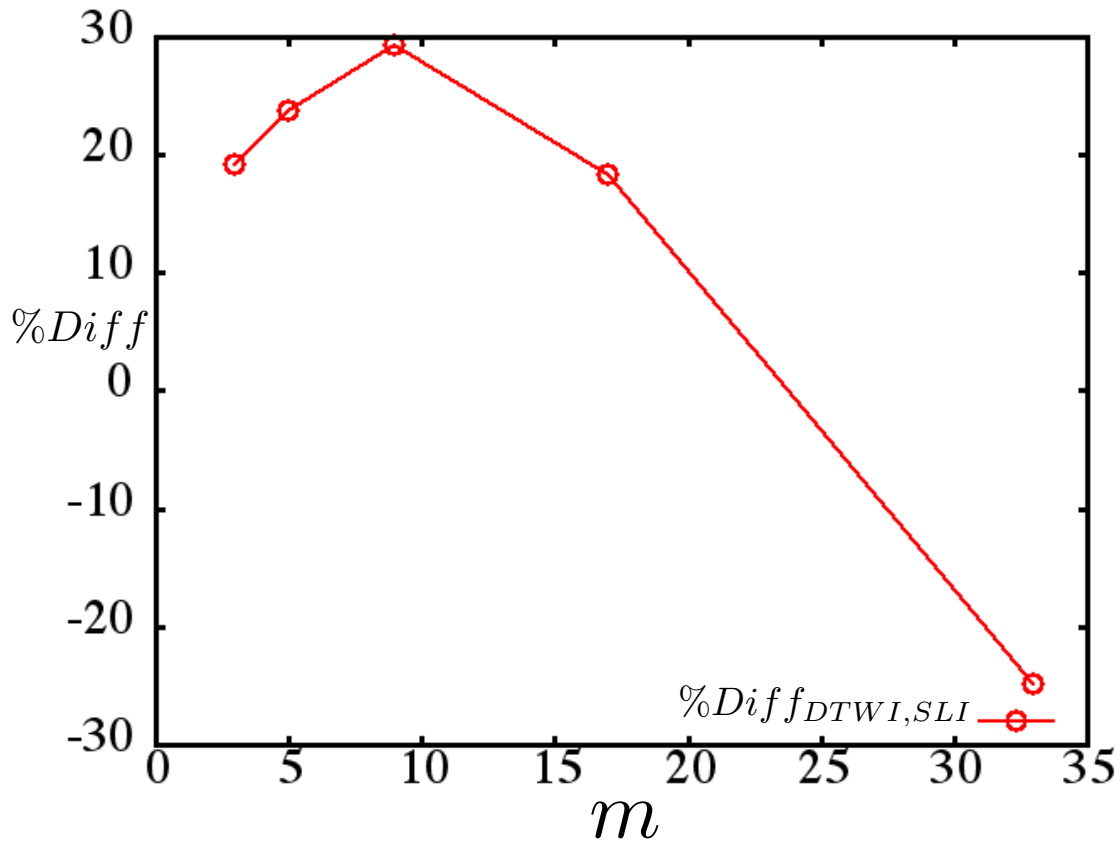

Figure 25: The figure represents the percentage difference $\%Diff_{DTWI,SLI}$ between Err^2_{SLI} and Err^2_{DTWI} for the value of $m = 3, 5, 9, 17, 33$. For the fourth one, the DTWI strategy is $\sim 20\%$ better than the SLI technique.

Fig. 24 does not show the interpolation when the number of known sequences is two, because the distance between them is large. It is an extreme case where any kind of interpolation would be inconsistent. In Figure 26, we present the results of Err^2_{DTWI} and Err^2_{SLI} obtained for each interpolated sequence. We observe that the DTWI interpolates better the most of the sequences than the SLI technique.

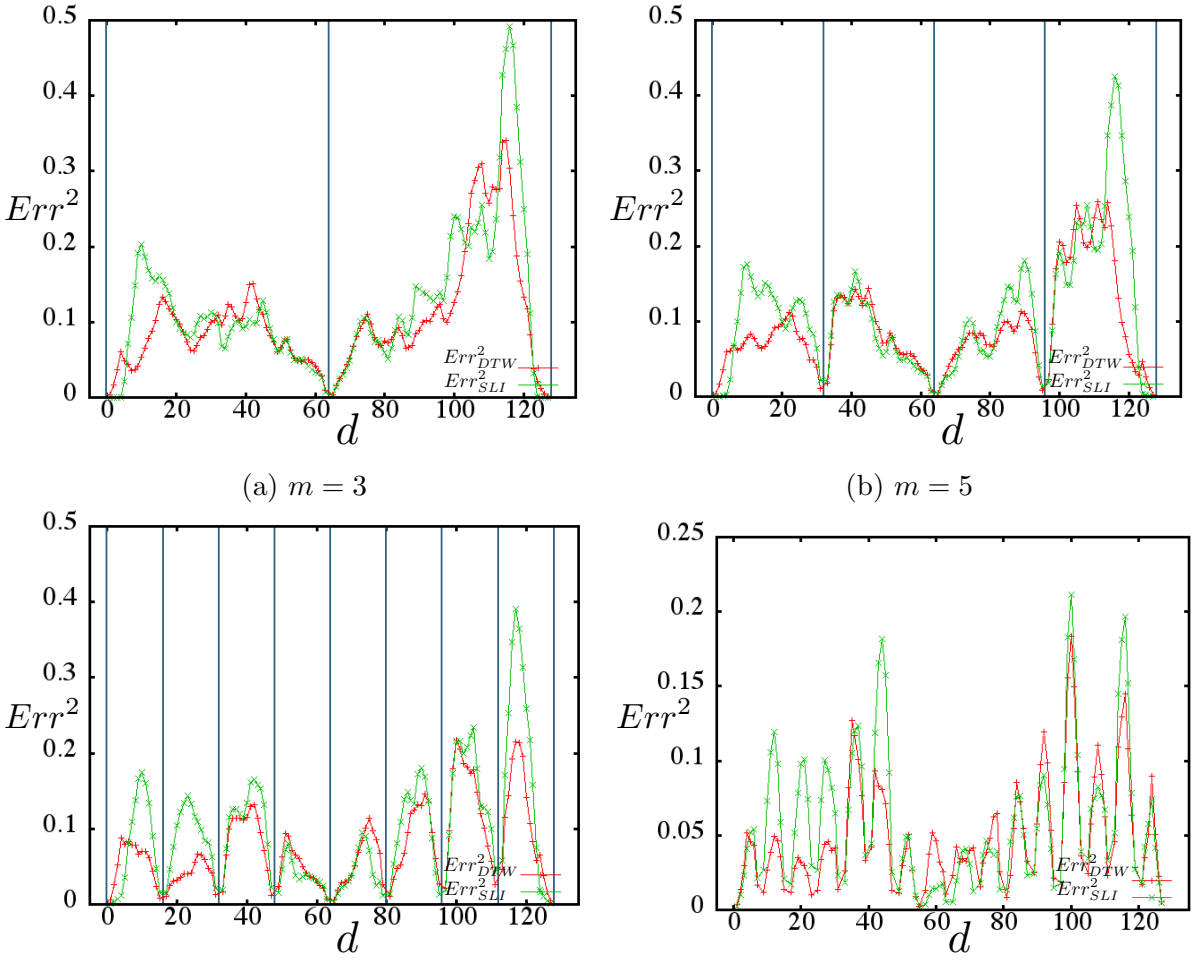

(a) $m = 3$

(b) $m = 5$

(c) $m = 9$

(d) $m = 17$

Figure 26: For $m = 3, 5, 9, 17$, the figures represent the variation of the Err^2_{DTWI} and the Err^2_{SLI} in function of the distance d from the first sequence, in other words, for the cases where the DTWI is better than the SLI technique. The blue vertical lines represent the known sequences when $m = 3, 5, 9$. When $m = 17$ there are not blue lines because the distance among them is too small to be represented.

4 CONCLUSION

In the Chapter 3, we presented a technique introduced in 1978, by H. Sakoe and S. Chiba in a study about spoken word recognition, called Dynamic Time Warping (DTW) [23]. The DTW allows us to relate two correlated temporal sequences, $f_1(i)$ and $f_2(j)$ where $i, j \in [1 : N]$. The construction of a cost matrix, formed by the elements $p(i, j) = |f_1(i) - f_2(j)|$, and the following search for an optimal warping path between the element in position $(1, 1)$ and (N, N) of that matrix lead us to find the global similarities between the two sequences.

Next, we introduced our interpolation method starting from the description of the problem we wanted to solve. We used a seismic landscape formed by 129 depth-dependent sequences of length 201. Specifically, we applied the Dynamic Time Warping Interpolation (DTWI) to interpolate the unknown sequences existent between two known sequences. This operation was repeated for different values of known sequences m, where $m = 2, 3, 5, 9, 17, 33, 65$. The same operation was performed using a Standard Linear Interpolation (SLI). The two results obtained were compared through the calculation of the square errors Err^2_{DTWI} and Err^2_{SLI}. Both the square errors were calculated comparing the simulated data with the remaining real data from the seismic landscape. We obtained a better interpolation, using the DTWI, for the values of $m = 3, 5, 9, 17$. Specifically, for those cases, the percentage difference between them was $\sim 20\%$ in favor of the DTWI. We conjecture that our strategy works better when the horizontal pattern of the soil has the same order size of the distance between the sequences considered in the DTWI.

As a perspective for future work, we intend to extend our interpolation strategy to three dimensions using data from soil drilling. The soil drilling data are more available, as it is not the result of the waves' reflection and refraction, since they are taken onsite. A three-dimensional analysis is possible when we have three sequences correlated with each other. Another proposal is to apply an extension of the DTW recently developed by S. M. Hope *et al.* called Global Correlation Analysis (GCA) [24]. While the DTWI gives us an univocal correspondence between the elements of the two sequences, the GCA scheme

gives us several correspondences and it can order them by importance.

BIBLIOGRAPHY

[1] S. N. Dorogovstev, J. F. F. Mendes. Evolution of Networks. *Adv. Phys.,* 51, 1079, 2002.

[2] Bar-Yam, Yaneer. *General features of Complex Systems, Encyclopedia of Life Support Systems* . Oxford: UNESCO Publishers, 2002.

[3] M. E. J. Newman. *Networks: An Introduction*. United Kingdom: OXFORD University Press, 2010.

[4] Albert-László Barabási. *Linked*. USA: Plume, 2003.

[5] B. B . Mandelbrot. *How long is the coast of Britain? Statistical self-similarity and fractional dimension*. Science: 156, 636-638, 1967.

[6] C. C . Barton, P. R. La Pointe. *Fractals in Petroleum Geology and Earth Processes*. USA: Springer, 1995.

[7] B. B . Mandelbrot. Self-Affine Fractals and Fractal Dimension. *Physica Scripta,* 32, p. 257-260, 1985.

[8] M. F. Barnsley, R. L. Devaney, H. Peitgen, D. Saupe, R. F. Voss, B. B . Mandelbrot. *The science of Fractal Images*. Springer: Heiz-Otto Peitgen and Dietmar Saupe, 1988.

[9] B. B . Mandelbrot. *The Fractal Geometry of Nature*. New York: W. H. Freeman, 1982.

[10] Harry Kesten. *Percolation Theory for Mathematicians*. Paris: P. Huber and M. Rosenblatt, 1975

[11] B. B . Mandelbrot. *Les Objects Fractals: Forme, hasard et dimension*. Paris: Flammarion, 1982.

[12] McGraw-Hill. *Concise Encyclopedia of Science and Technology, 5th*. United States of America: RR Donnelley, 1987.

[13] J. Feder. *Fractals*. New York:Plenum Press,1988.

[14] A. Lakhtakia, R. Messier, V. V. Varadan, V. K. Varadan. Self-similarity versus self-affinity: the Sierpinski gasket revisited. *J. Phys. A,* 19, L985-L989, 1986.

[15] B. B . Mandelbrot. *Fractal and Chaos: the Mandelbrot Set and Beyond*. New York: Springer, 2004.

[16] D . Stauffer, A. Aharony. *Introduction to percolation theory*. London: Taylor and Francis, 1995.

[17] S . R. Broadbent and J . M. Hammersley. Percolation processes. *Mathematical Proceedings of Cambridge Philosophical Society,* 53, L629-L641, 1957.

[18] Erneson Alves de Oliveira. *Linhas divisoras de àguas e fraturas de caminhos òtimos em meios desordenados*. Fortaleza: Universidade Federal do Ceara, 2012.

[19] W. D. Wallis. *A Beginner's Guide to Graph Theory*. USA: Birkhäuser, 2000.

[20] T. H. Cormen, C. E. Leiserson and R. L. Rivest. *Introduction to algorithms*. Cambridge: McGraw-Hill Book Company and The MIT press, 1990.

[21] E . W. Dijkstra. A Note on Two Problems in Connexion with Graphs. *Numerische Mathematik,* 1, 269-271, 1959.

[22] M. Muller. *Information Retrieval for Music and Motion*. Germany: Springer, 2007.

[23] H . Sakoe, S . Chiba. Dynamic Programming Algorithm Optimization for Spoken Word Recognition. *IEEE Transaction on Acoustics, Speech, and Signal Processing,* 1, ASSP-26, 1978.

[24] S . M . Hope, A . A . Moreira, J . S . Andrade Jr, A . Hansen. Reservoir mapping by global correlation analysis. *International Journal of Rock Mechanics and Mining Sciences,* 67, 181-183, 2014.